

**NON-LINEAR SYSTEMS ANALYSIS  
IN ELECTRO-RETINOGRAPHY**

**NON-LINEAR SYSTEMS  
ANALYSIS IN  
ELECTRO-RETINOGRAPHY**

A. TROELSTRA



**INSTITUTE FOR PERCEPTION RVO-TNO**

**NATIONAL DEFENCE RESEARCH ORGANIZATION TNO**

**SOESTERBERG - THE NETHERLANDS**

*Gedrukt ter Koninklijke Drukkerij Van Gorcum & Comp.*

## PREFACE

Electro-retinography is one of those research tools which present objective information about the function of the visual system. It records the integrated effect of diffuse and complex actions of the retinal nervous system. Obviously no other approach to the intact system is available but input-output system analysis. In spite of the work by quite a number of people the present picture of it is still far from complete. It has, however, grown considerably in the last decade by the type of system analysis as introduced by de Lange for physiological mechanisms. With his work on the psychophysics of flicker he opened a new way to the play grounds -also of electrophysiology. His analysis in terms of amplitude-frequency and phase-frequency dependencies of linearly acting decisive components in the systems, is based on experiments with sinusoidally modulated stimuli. His work did initiate and propagate in laboratories all over the world a wave of "sinism" in stimulus design that interfered and for a good deal overruled the "cubism" of the earlier commonly used square-shaped all-none inputs. The activities of the "sinist's" proved to be quite profitable and they still are so, as far as the underlying ground for their devotion to, or assumption of, linearity turns out to be firm. Essentially, linearity means that the response function to simultaneously applied input components is the arithmetic sum of the respective responses. In a way therefore it was against the spirit of the times when Troelstra and Schweitzer started their electro-retinographic studies in a program of non-linear system analysis. This could be justified though, as it was known for long that the visual system contains non-linear aspects. Provided that the existent non-linearities were amplitude dependent only, the dependencies of output-amplitude on both frequency and intensity of sinusoidal stimulation would suffice for full description of the system. From adaption phenomena presented in Chapter III it appears, however, that this hypothesis is not sustainable.

In the reported study a non-linear system is put forward by which stimulus and response are linked together in the time-domain. The model predicts the response to any single stimulus as it is demonstrated for block-, step- and rampfunctions as well as for repetitive stimuli including sinusoidally modulated light. For the latter stimuli phase- and amplitude-frequency characteristics were calculated from the model and verified experimentally. The drastic change in appearance of the ERG to a flash when the eye is in a steady moderately light adapted state, in stead of being completely dark adapted, also proved to follow from the model.

An important conclusion from the underlying work asks special attention. I here have in mind the author's claim that Talbot's law – response to an intermittent stimulus above the critical flicker fusion, appears like the response to a constant stimulus of the same time-averaged intensity – is valid for his particular model in which a non-linear component operates first on the stimulus followed by a linear operation in a second stage. This defies the conception of several authors who used Talbot's law in order to show that before the signal reaches non-linear elements it has been subjected to an attenuation in a lowpass filter.

Although the model is purely operational in nature, similarity between properties of components of the model and of properties of visual functions as apparent from psychophysical experiments might be more than merely accidental. The final remarks in the author's last chapter on the relationship between his suggest model and some results of psychophysical studies that a new opening towards promising fields of exploration has been found.

MAARTEN A. BOUMAN

## CONTENTS

CHAPTER I	REVIEW AND INTRODUCTION . . . . .	1
CHAPTER II	NON-LINEAR SYSTEMS ANALYSIS . . . . .	5
	A. Introduction . . . . .	5
	B. A special type of non-linear behaviour . . . . .	6
	C. Sinusoidal stimulation . . . . .	11
	D. Summary . . . . .	12
CHAPTER III	SOME FUNDAMENTAL PROPERTIES OF THE RELATION BETWEEN THE ELECTRO-RETINOGRAM AND THE STIMULUS CONDITIONS . . . . .	13
	A. Introduction . . . . .	13
	B. Characterization of the system . . . . .	14
	C. Determination of the characteristic functions $e$ , $S$ and $g$ of the electro-retinographic system. . . . .	18
CHAPTER IV	PREDICTED AND EXPERIMENTAL RESULTS FOR SINGLE STIMULI . . . . .	27
	A. Amplitude of the $B_g$ -wave as a function of the stimulus duration for block-shaped stimuli. . . . .	27
	B. The step-function response . . . . .	32
	C. The ramp-function response . . . . .	38
	D. Analysis of an arbitrary response . . . . .	41
	E. Conclusion . . . . .	41
CHAPTER V	PREDICTED AND EXPERIMENTAL RESULTS FOR REPETITIVE STIMULI . . . . .	44
	A. Short flashes with low repetition frequencies . . . . .	44
	B. Short flashes with high repetition frequencies . . . . .	52
	C. Sinusoidal stimulation . . . . .	53
	D. The behaviour of the light-adapted eye . . . . .	64
CHAPTER VI	DISCUSSION . . . . .	68
SUMMARY . . . . .		75
SAMENVATTING . . . . .		77
REFERENCES. . . . .		80

## CHAPTER I

### REVIEW AND INTRODUCTION

The electro-retinogram (*ERG*) has been studied for about one hundred years, since Holmgren<sup>22</sup> first recorded the change in electrical potential from the eye upon stimulation with light. Not much attention was paid to these experiments until the independent rediscovery of electro-retinography in 1873 by Dewar and McKendrick<sup>13</sup>. They found that an isolated frog retina could produce the same electrical response as the intact eye. This demonstrated that the electro-retinogram is generated in the first place in the retina itself, and not in some other part of the eye.

Dewar and McKendrick<sup>13</sup> also found that the amplitude of the electrical response in animals is more or less proportional to the logarithm of the stimulus intensity (Weber's law). Adaption to light decreased the response amplitude, while dark-adaptation increased this amplitude (Kühne and Steiner<sup>27</sup>). Furthermore, it was found that those wavelengths which appear brightest to the human eye evoked the highest electrical responses (Dewar and McKendrick<sup>13</sup>, Holmgren<sup>22</sup>). Thus a relationship between the *ERG* and the subjective impression of vision was suggested, and much research has since been done in this direction.

In general the idea has been to use the *ERG* on one hand in psychophysics as an objective response criterion, and on the other hand as a diagnostic tool for clinical use. Further experiments indicated, however, that the relationship between the *ERG* and visual processes is an indirect and complicated one.

The responses noted by earlier investigators were distorted due to poor electrodes and recording techniques. Gotch<sup>16</sup>, in 1903, was the first one who obtained fairly undistorted records. Further improvement was made by Brücke and Garten<sup>8</sup> in 1907 using a string galvanometer. It was then possible to pay more attention to the wave-form of the responses, and in 1908 Einthoven and Jolly<sup>14</sup> presented their

historical analysis of the *ERG* into components. This was followed by other component-analyses by Waller<sup>41</sup> in 1909, by Piper<sup>29</sup> in 1911 and by Granit<sup>19</sup> in 1933. Granit's<sup>19</sup> analysis became the most important and well-founded one, for he showed selective effects of certain drugs upon each of his components.

However, even now there is a lack of basic understanding of the relationship between the light stimulus and the *ERG*. We quote Johnson<sup>23</sup> (1958): "The purposes of all these will be best served if the attention of experimenters can be centered on the task of producing an accurate, detailed picture of the forms and variations of response correlated with major stimulus variables. Not until these various parameters have been adequately cataloged will we be able to select the most suitable conditions for observing particular aspects of the response or to suggest standard conditions for clinical use."

These words express the basic motivation underlying this thesis.

An obvious step forward would be an attempt to find a mathematical description for the system one can think of as existing between light-input and *ERG*-output. Since such a system is constructed merely on the basis of an input-output analysis, the parameters defining the system do not necessarily have to be related to the real physiological properties of the eye.

A nice example of such an approach is given by the attenuation characteristics of De Lange<sup>11</sup>. Here the input to the eye is an illuminated background, the intensity of which is sinusoidally modulated with a low modulation percentage. The output criterion is the critical flicker fusion frequency. The assumption is made that for such relatively small variations, the eye acts as a linear system. The same small-signal-linearisation has been applied to the electro-retinographic system by v. d. Tweel<sup>37</sup>. If for instance the non-linearity depends on the amplitude of the input only (e.g. a saturation effect), the relation between the output  $R(t)$  and the input  $I(t)$  can, in general, be written as:

$$R(t) = F[I(t)],$$

where  $F$  is some non-linear function independent of the time  $t$ .

For an input  $I(t) = I_0 + i(t)$  the output is equal to:

$$F[I_0 + i(t)] = F(I_0) + \frac{\delta F}{\delta I_0} i(t) + \frac{1}{2} \frac{\delta^2 F}{\delta I_0^2} i^2(t) + \dots \quad (1)$$

If we neglect the constant term and also assume that  $i^2(t) \ll i(t)$



according to small-signal-linearisation techniques, then Eq. (1) transforms into:

$$R(t) = \frac{\delta F}{\delta I_0} i(t),$$

which is a linear relation.

It should be noted that the validity of small-signal-linearisation on the basis of the relation  $i^2(t) \ll i(t)$  alone, can be justified in this way only for amplitude dependent non-linearities. A further disadvantage of small-signal-linearisation is that it describes the system under rather restricted conditions, while leaving quite important non-linear response characteristics out of consideration.

For these reasons we intentionally turn directly in this thesis to a fundamentally non-linear model, that focuses attention at the crucial non-linear properties of this interesting biological system.

In order to orient the reader, we include in this chapter a brief description of the experimental arrangement. A schematic diagram is shown in Fig. 1.

A projection TV tube produces a light spot on its face and the intensity of this spot can be varied in proportion to the grid-voltage. The spot is projected via the condenser  $C_1$ , filter  $F_1$ , half-mirror  $H_1$ , and condenser  $C_2$  onto the plane of the pupil. Thus the light spot is seen by the eye in Maxwellian view and the circular field subtends a solid angle of about thirty degrees. At the same time a fixation diaphragm  $D$  is imaged via the lens  $L$ , the half-mirror  $H_1$  and the condenser  $C_2$  onto the retina of the eye which is accommodating at infinity.  $F_1$  consists of a set of neutral density filters and a colour filter.

In all our experiments we used human subjects, situated in an electrically shielded room. The electro-retinogram is detected using one Riggs-type contact-lens silver-electrode and two silver skin-electrodes placed on the forehead of the subject. The electrical signal is then fed into a chopper amplifier with differential input. The chopper amplifier has a frequency range from 0 to 90 cps (3 dB). To avoid a slow zero drift of the electrodes a series capacitor was sometimes used in the input leads to the amplifier. The resulting time constant of the input circuit was always 2 sec or longer, and will be specified in every particular situation. The output signal of the chopper amplifier is displayed on an oscilloscope for monitoring purposes and recorded on a multi-channel pen-recorder together with the light stimulus, which is continuously measured by a photocell.

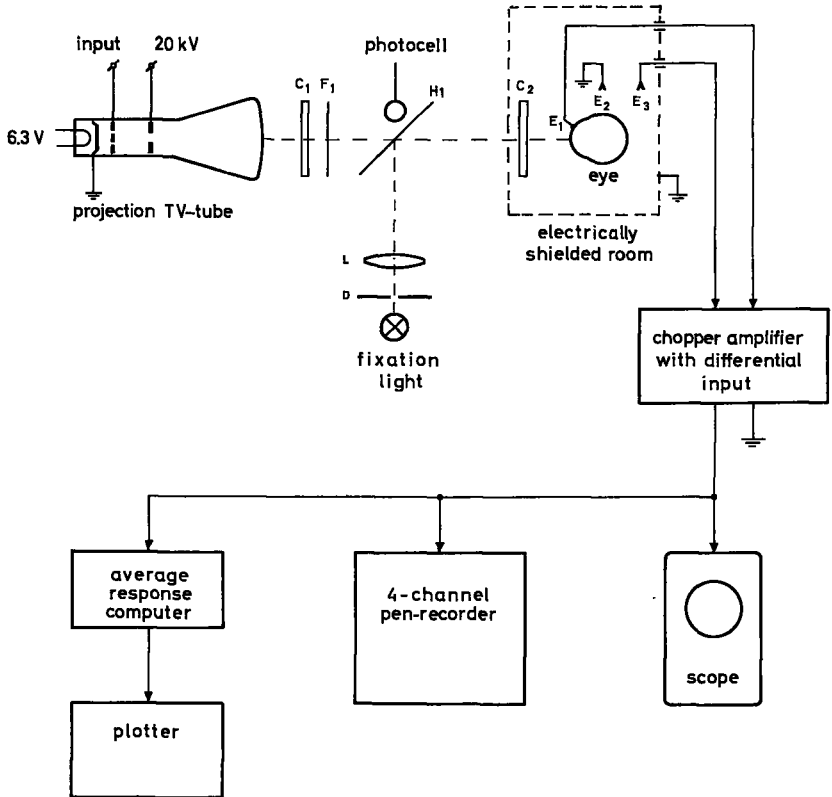


Fig. 1 - Schematic diagram of the experimental arrangement.

When the signal-to-noise ratio is low, many responses to identical stimuli are averaged by means of an average response computer\*. By this procedure the signal-to-noise ratio is improved with a factor equal to the square root of the number of averaged responses, providing always that the system is maintained in a stationary state.

\* The first measurements were made with an average response computer developed and built in our laboratory by Mr. Huistra and Mr. Schipper. This machine had a core memory of 250 words of 16 bits each, in connection with a 6 bit 10kc analog-to-digital converter. Later on the Mnemotron CAT average response computer was used, which had become commercially available by that time.

## NON-LINEAR SYSTEMS ANALYSIS

## A. Introduction

It is well known that in general systems analysis the important distinction is made between linear and non-linear systems. The first group can be treated mathematically in a rather easy way because of the superposition principle. For the second group, however, no straightforward analysis exists, and under restricted conditions only some kinds of non-linearities can be described satisfactorily in a mathematical way. In this respect two methods are of special importance, namely the describing function analysis and the phase-plane analysis. The describing function analysis was developed in the USA by R. J. Kochenburger<sup>26</sup> and is based on the following three assumptions<sup>36</sup>:

1. All non-linear components in the system can be taken together and are considered as one non-linear element.
2. The output of the non-linear element depends only on the present value and past history of the input.
3. If the input of the non-linear element is a sinusoidal signal, only the fundamental component of the output is of significance for further system operation.

If these three assumptions are satisfied, the describing function  $N$  of the non-linear element is defined as  $N = \frac{C_1}{R}$ , where  $R$  is the amplitude of the sinusoidal input signal  $R \sin \omega t$ , and  $C_1$  is the amplitude of the fundamental output component. For any non-linear system  $N$  will necessarily depend on the amplitude  $R$ . Moreover, if the non-linear system contains energy storage elements,  $N$  will depend on the frequency  $\omega$ . In addition  $N$  may be real or contain a phase shift. The describing function analysis can be applied to systems of any order, and describes the system behaviour in the frequency domain\*.

\* The order of a system refers, in general, to the order of the differential equation which describes the relation between input and output of the system.

The phase-plane method, however, can only be applied easily to second order systems, where it may be used to study the transient behaviour of a system subject to initial conditions but otherwise unexcited. In general, only signal-dependent non-linearities are admitted, and time-dependent systems, or systems with parameters varying with time, are excluded.

Starting point for the phase-plane analysis is a second order differential equation of the type:

$$\ddot{x} + a(\dot{x}, x)\dot{x} + b(\dot{x}, x)x = 0, \text{ where } a(\dot{x}, x) \text{ and } b(\dot{x}, x)$$

are functions of the signal and its derivative. The phase-plane is a plot of  $\dot{x}$  as a function of  $x$ .\*

From the foregoing it is clear that a rather detailed knowledge of the internal system parameters is necessary before this type of analysis can be applied. Finally, the phase-plane analysis describes the system behaviour in the time domain only.

#### B. A special type of non-linear behaviour

For some non-linear systems the describing function analysis can be modified to give the system behaviour in the time domain as well as in the frequency domain.

We will concern ourselves with systems where the momentary input  $I(t)$  at time  $t$  is multiplied by a function  $S$  depending on the past history of the input and the time  $t$ , in order to get the output. Hence the output  $H(t)$  of the non-linear element can be written as:

$$H(t) = I(t)S \tag{2}$$

An example of such a system may be a system which is insensitive just after a strong input but which becomes more and more sensitive during the time in which no input is presented. Moreover, the degree of insensitivity may depend on the amplitude and duration of the input.

A system which shows these properties is often difficult to analyse with sinusoidally modulated inputs, because in that situation the

\* The signal  $x$  can be for instance the output of a system, or the error signal in a feedback system. Curves in the phase-plane indicate the time variations of  $x$  and  $\dot{x}$ . The initial conditions  $x(0)$  and  $\dot{x}(0)$  locate a point in the phase-plane, while the path through this point indicates the system behaviour at all later times.

system is operating in a rather insensitive state. One would rather stimulate such a system with impulses or step-functions.

Now we make the following assumption: the past history of the input as far as the function  $S$  is concerned, can be described by a weighting function  $g(t)$ . This means that  $S$  can be written as:

$$S = S \left[ \int_0^t I(\tau)g(t - \tau)d\tau \right] \text{ with } g(x) = 0 \text{ for } x \leq 0 \quad (3)$$

If, for instance, the weighting function is a delta-function, then  $S \left[ \int_0^t I(\tau)\delta(t - \tau)d\tau \right]$  becomes  $S \left[ \frac{1}{2} I(t) \right]$ , in other words,  $S$  would depend on the amplitude of the input signal only.

The problem now is how to analyse a system consisting of a combination of a linear element  $l$  and a non-linear element  $n$ , if besides this it is known that the non-linearity of  $n$  can be described by a set of equations analogous to Eq. (2) and (3). There are two possibilities as shown in Fig. 2a and b.

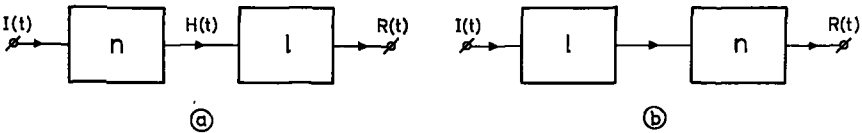


Fig. 2 - Possible arrangements of the non-linear and linear elements.

With an arrangement as in Fig. 2b it is, in general, impossible to determine the characteristics of the linear element (for instance the impulse response  $e(t)$ ) and the non-linear element (the functions  $S$  and  $g$ ), from a simple input-output analysis. However, it is possible to determine a describing function  $N$  for the system as a whole which describes the system behaviour for sinusoidal inputs.

With the arrangement of Fig. 2a the linear and non-linear characteristics of  $l$  and  $n$ , respectively, can be found. We will show for the case 2a how to determine the impulse response  $e(t)$  of  $l$  and the functions  $S$  and  $g$  characterizing  $n$ , from an input - output analysis.

The relation between the output  $R(T)$  and the input  $I(T)$  can be written as:

$$R(T) = \int_0^T I(t) S \left[ \int_0^t I(\tau)g(t - \tau)d\tau \right] e(T - t)dt \quad (4)$$

It is assumed that there has been no input before  $t = 0$ , in other words  $I(t) = 0$  for  $t < 0$ .

First the system is to be stimulated with short impulses of amplitude  $I_0$  and duration  $T_0$ . The duration is to be short as compared with any time constant in the resulting response. Then Eq. (4) becomes:

$$R(T) = \left\{ \int_0^{T_0} I(t) S \left[ \int_0^t I(\tau) g(t - \tau) d\tau \right] dt \right\} e(T)$$

or

$$R(T) = \left\{ I_0 \int_0^{T_0} S \left[ I_0 \int_0^t g(t - \tau) d\tau \right] dt \right\} e(T) \quad (5)$$

Now the assumption is made that  $g$  does not change significantly during the short time  $T_0$ . Then Eq. (5) transforms into:

$$R(T) = \underbrace{\left\{ I_0 \int_0^{T_0} S [I_0 t g(0)] dt \right\}}_k e(T) \quad (6)$$

The term  $k$  does not depend on  $T$ . In this situation the response  $R(T)$  is a constant times the impulse - response  $e(T)$  of the linear element. In other words the impulse-response  $e(T)$  can be found from Eq. (6), after measurement of  $R(T)$ .

Now we suppose that  $k$  is known as a function of the amplitude of the input  $I_0$ .

Hence 
$$k(I_0) = I_0 \int_0^{T_0} S [I_0 t g(0)] dt \quad (7)$$

This can be transformed into:

$$k(I_0) = \int_0^{I_0 T_0} S [x g(0)] dx \text{ with } x = I_0 t$$

Differentiating both sides with respect to  $I_0$ :

$$S [I_0 T_0 g(0)] = \frac{1}{T_0} \frac{dk}{dI_0} \quad (8)$$

From Eq. (8)  $S$  can be determined.

Finally, we will indicate how the weighting function  $g(t)$  can be found. The system is stimulated with double-pulses as shown in Fig. 3. Again the duration  $T_0$  is to be short as compared with any time -

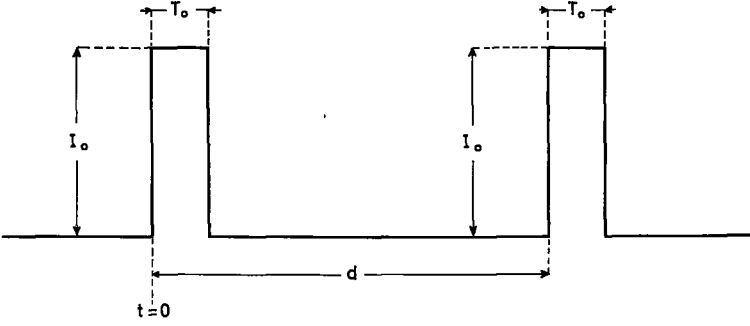


Fig. 3 - Double-pulse.

constant in the resulting response. According to Eq. (4) the response can be written as:

$$R(T) = I_0 \int_0^T S [I_0 \int_0^t g(t - \tau) d\tau] e(T - t) dt \quad (9)$$

Here we must take into account that  $I_0 = 0$  for  $t < 0$ , for  $T_0 < t < d$  and for  $t > d + T_0$ .

Now we separate in the response  $R(T)$  the two contributions  $R_1(T)$  and  $R_2(T)$  of the first and second impulse, respectively.

$$\text{Consequently } R(T) = R_1(T) + R_2(T) \quad (10)$$

Combining Eq. (9) and (10) we get:

$$R_1(T) + R_2(T) = \{I_0 \int_0^{T_0} S [I_0 \int_0^t g(t - \tau) d\tau] dt\} e(T) + \\ + \{I_0 \int_d^{d+T_0} S [I_0 \int_0^t g(t - \tau) d\tau] dt\} e(T - d)$$

According to Eq. (5) and (6) this can be written as:

$$R_1(T) + R_2(T) = k(I_0) e(T) + \{I_0 \int_d^{d+T_0} S [I_0 \int_0^t g(t - \tau) d\tau] dt\} e(T - d)$$

Working out of the last term in this equation results in:

$$R_1(T) + R_2(T) = k(I_0) e(T) + \\ + \{I_0 \int_d^{d+T_0} S [I_0 T_0 g(d) + I_0(t - d)g(0)] dt\} e(T - d)$$

or

$$R_1(T) + R_2(T) = k(I_0)e(T) + \left\{ \int_{I_0 d}^{I_0(d+T_0)} S[I_0 T_0 g(d) + xg(0) - I_0 d g(0)] dt \right\} e(T - d)$$

where  $x = I_0 t$

Now the substitution  $y = I_0 T_0 \frac{g(d)}{g(0)} + x - I_0 d$  is made.

This yields:

$$R_1(T) + R_2(T) = k(I_0)e(T) + \left\{ \int_{I_0 T_0 \frac{g(d)}{g(0)}}^{I_0 T_0 \left(\frac{g(d)}{g(0)} + 1\right)} S[yg(0)] dy \right\} e(T - d)$$

This integral can be found with Eq. (8):

$$R_1(T) + R_2(T) = k(I_0)e(T) + \left\{ k[I_0 T_0 \frac{g(d)}{g(0)} + I_0 T_0] - k[I_0 T_0 \frac{g(d)}{g(0)}] \right\} e(T - d) \quad (11)$$

From Eq. (11) we see that the amplitude of the response  $R_1(T)$  evoked by the first impulse is equal to  $k(I_0)$ . The amplitude of the second response is equal to:

$$k[I_0 T_0 \frac{g(d)}{g(0)} + I_0 T_0] - k[I_0 T_0 \frac{g(d)}{g(0)}]$$

Both responses have the same shape, the second response only starts  $d$  seconds after the first one.

To determine the function  $g(d)$  experimentally an experiment can be done where the system is stimulated with double-pulses of a fixed amplitude  $I_0$ . The amplitude of the second response is determined for various separations  $d$  of the double-pulses. If the two responses do not overlap this is no problem at all. If they do overlap the response to the second impulse can be found by subtracting the response to the first impulse alone from the response to the two impulses together.

Finally, the amplitude of the second response is equalized to

$k[I_0 T_0 \frac{g(d)}{g(0)} + I_0 T_0] - k[I_0 T_0 \frac{g(d)}{g(0)}]$ , from which the factor  $\frac{g(d)}{g(0)}$  can be solved, since  $k(I)$  is supposed to be known. In this way  $g(d)$  is found, except for the constant  $g(0)$ .



### C. Sinusoidal stimulation

If a system which can be described by Eq. (4) is stimulated with a sinusoidal input  $I_0 (1 + \rho \sin \omega t)$ , the output is equal to:

$$R(T) = I_0 \int_0^T (1 + \rho \sin \omega t) S \left[ I_0 \int_0^t (1 + \rho \sin \omega \tau) g(t - \tau) d\tau \right] e(T - t) dt \quad (12)$$

In general,  $R(T)$  will contain the fundamental frequency plus all higher harmonics. To analyse the fundamental frequency in  $R(T)$  in terms of gain and phase-shift with respect to the input, Eq. (12) is separated into two parts.

$$R(T) = I_0 \int_0^T H(t) e(T - t) dt \quad (12a)$$

$$H(t) = (1 + \rho \sin \omega t) S \left[ I_0 \int_0^t (1 + \rho \sin \omega \tau) g(t - \tau) d\tau \right] \quad (12b)$$

Since Eq. (12a) describes a linear system, the only term in  $H(t)$  which contributes to the fundamental frequency in  $R(T)$  is of the same frequency. Therefore, the first step is to solve Eq. (12a) for  $H(t) = A \sin \omega t$ .

This is a common problem in control theory. If  $e(T - t)$  can be approximated by an algebraic function, the integral in Eq. (12a) may be found in some particular cases. If  $e(T - t)$  is only known in a graphical form, the impulse method of Guillemin<sup>36</sup> or the graphical method of Solodovnikov<sup>33</sup> may be applied. The impulse method of Guillemin will be worked out more extensively in a later chapter.

Thus it is always possible to write  $R(T)$  in the form:

$$R(T) = B(\omega) \sin [\omega t + \varphi(\omega)], \quad (13)$$

where  $B(\omega)$  is the frequency-dependent gain and  $\varphi(\omega)$  the frequency-dependent phase-shift of the linear system.

After this the second step is to solve Eq. (12b). Therefore, it is necessary to have some specific knowledge about the functions  $S$  and  $g$ , which can be obtained from experiments with short single and double pulses as described before. Then the integral  $\int_0^t (1 + \rho \sin \omega \tau) g(t - \tau) d\tau$  can be solved in the same way as in Eq. (12a).

Finally, we can write the solution of Eq. (12b) in the general form:

$$\begin{aligned}
H(t) = & C(I_0, \omega) + D(I_0, \omega) \sin [\omega t + \varphi_1(I_0, \omega)] + \\
& + E(I_0, \omega) \sin [2\omega t + \varphi_2(I_0, \omega)] + \dots \quad (14)
\end{aligned}$$

Combining Eq. (13) and (14), we find for the total gain and phase-shift of the fundamental component in the response  $R(T)$ :

$$\text{total gain} = B(\omega) \times D(I_0, \omega) \quad (15)$$

$$\text{total phase-shift} = \varphi(\omega) + \varphi_1(I_0, \omega) \quad (16)$$

#### D. Summary

A method of analysing a special type of non-linearity is shown. The non-linear operation consists of multiplication of the input  $I(t)$  by the function representing the non-linear element; this function is a variable sensitivity  $S$ , which depends on the past history of the input  $I(t)$ . The particular dependence on the past history of the input is specified by the weighting function  $g$ . The non-linear element may be followed by a linear element. The output of the non-linear element is given by:

$$I(t)S \left[ \int_0^t I(\tau)g(t - \tau)d\tau \right]$$

The impulse response of the linear element is given by  $e(t)$ .

By stimulating the system as a whole with single impulses of short duration  $T_0$  and various amplitudes  $I_0$ , the impulse response of the linear element and the function relating the height of the response and the impulse-amplitude  $k(I)$  can be determined. From this function  $k(I)$  the function  $S$  can be derived.

If the system is stimulated with double-pulses with various separations between the two pulses, the function  $g$  can be found from the height of the second response.

After this it is shown how the gain versus frequency and phase versus frequency of the fundamental component can be calculated in the case of sinusoidal stimulation.

**SOME FUNDAMENTAL PROPERTIES OF THE RELATION  
BETWEEN THE ELECTRO-RETINOGRAM  
AND THE STIMULUS CONDITIONS**

**A. Introduction**

In this chapter we will investigate the relation between some parameters in a light stimulus and the resulting electro-retinogram. The stimulus is supposed to be an intensity as a function of time:  $I(t)$ . The *ERG* depends on the stimulus conditions in a rather complicated way. The measurements concerning this subject in the literature can be divided into the following groups:

- a. The stimulus has a constant duration  $T_0$ , while the intensity  $I_0$  is variable, as shown in Fig. 4a.
- b. The stimulus has a constant intensity  $I_0$ , while the duration  $T_0$  is variable, as shown in Fig. 4b.
- c. The stimulus intensity is a more complicated function of time, as shown in Fig. 4c.
- d. The colour of the stimulus is variable.
- e. The area of the illuminated part of the retina is variable.

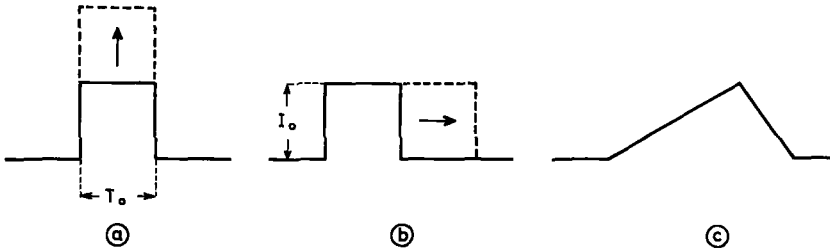


Fig. 4 - Various stimulus configurations.

In addition, the adaptive state of the eye may be varied, for instance, by a constant back-ground during the experiment, or by presenting the stimuli with a certain repetition rate.

The choice of so many variables makes it sometimes difficult or even impossible to compare various investigations in the literature. One of

the main reason is that the system: light stimulus  $\rightarrow$  *ERG* is basically non-linear, which makes the prediction of the result of a parameter variation difficult.

By applying the results obtained in the previous chapter for a special type of non-linear system, we will try to come to a more clear characterization of the electro-retinographic system.

### B. Characterization of the system

We look now more closely to what happens if, for example, short flashes (short as compared with the time-constants in the resulting response) are presented to a dark-adapted eye. We notice the following: At low intensities, the response consists of one slow positive wave, which is usually called the scotopic *B*-wave or  $B_s$ -wave. Positive always means: cornea positive with respect to the fundus of the eye. At moderate intensities this  $B_s$ -wave is preceded by a negative wave of shorter duration, the scotopic *A*-wave or  $A_s$ -wave.\*

At high intensities the shape of the *ERG* changes still further (Fig. 5). We will never go as high as those intensities, but restrict ourselves to small enough stimuli so that the response consists of an  $A_s$ -wave and  $B_s$ -wave only.

Moreover, we are particularly interested in the  $B_s$ -wave. Therefore, we always use a blue stimulus (max. at 460  $m\mu$ ) because of the relatively high blue sensitivity of this  $B_s$ -wave.

From Fig. 5 we notice that the non-linearity of the system light stimulus  $\rightarrow$  *ERG* results in a strong dependence of the shape of the *ERG* on the intensity of the stimulus. Over a large portion of the intensity range the amplitude of the response looks more like a logarithmic function of the intensity than a linear one. There occurs a delay time (or latency) between the beginning of the stimulus and the beginning of the response. This latency is intensity dependent, becoming shorter as intensity increases. Besides this, the amplitude of the response as well as the shape depend on the adaptive state of the eye.

Now there is an important observed property of the  $B_s$ -wave that

\* The nomenclature  $B_s$ -wave and  $A_s$ -wave of course refers to the scotopic system in vision. There are reasons to believe that such a classification is too simple and rather questionable. However, for the sake of conformity we will continue this nomenclature.

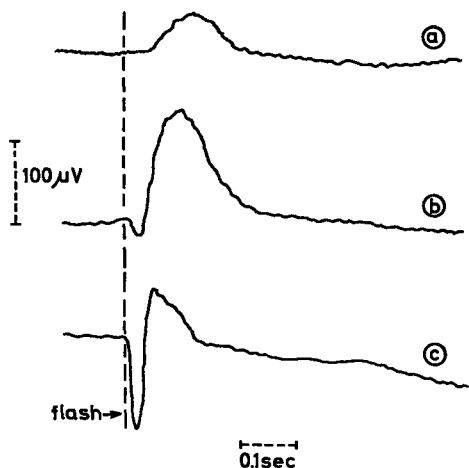


Fig. 5 - Three typical responses to stimuli of various intensities.

stimulus duration 100  $\mu$ sec

stimulus colour white

dark-adapted eye

dilated pupil

- a) Stimulus energy about  $3 \cdot 10^3$  times the absolute threshold.
- b) Stimulus energy about  $3 \cdot 10^4$  times the absolute threshold.
- c) Stimulus energy about  $3 \cdot 10^6$  times the absolute threshold.

enables an analogy to be made between it and the special non-linear system analysed in the previous chapter.

This property is, if a short stimulus, the intensity of which increases from zero up to a certain value, is presented to a dark-adapted eye, a range of intensities can be indicated, in which the resulting  $B_s$ -waves change only in amplitude, preserving their shape. This means that in this case the response may be written as:

$$\text{response as a function of time} = k \cdot u(t), \quad (17)$$

where  $u(t)$  represents some sort of unit-response, and  $k$  is the amplitude of the ERG.

$k$  depends on the intensity  $I$  of the stimulus. We will further elucidate this on the basis of Fig. 6 and 7.

In part a) of this figure the electro-retinographic responses are shown to a blue stimulus of a duration of 20 msec and relative intensities  $I = 300, 100, 30, 10, 3, 1$ .

In part b) of Fig. 6, the function  $k \cdot u(t)$  is plotted for various values of  $k$ , while  $u(t)$  is defined in Fig. 7. Any  $B_s$ -wave may be the basis for the construction of  $u(t)$ .

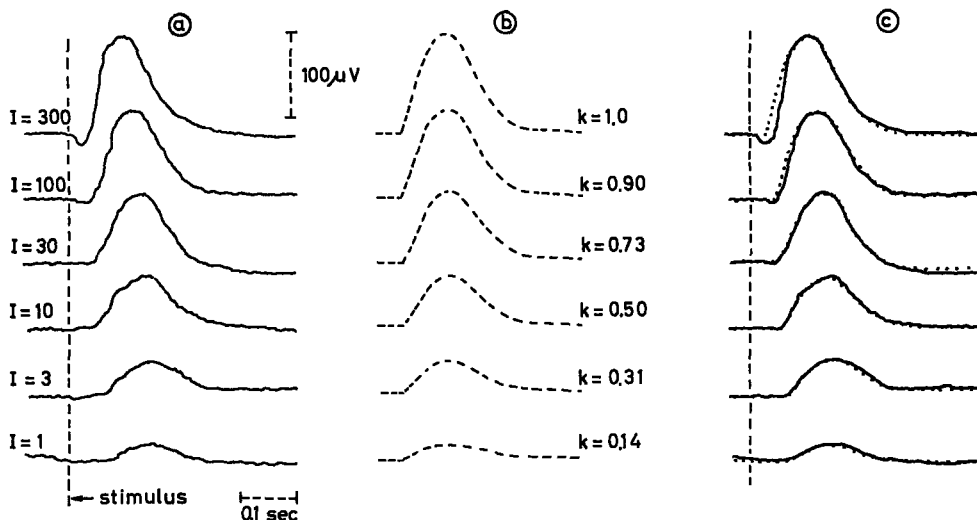


Fig. 6a - A series of ERG recordings obtained with short stimuli of various intensities (relative units).

b - The function  $k \cdot u(t)$  plotted for various values of  $k$ .

The unit-response  $u(t)$  is defined in Fig. 7.

The value of  $k$  in relative units.

c - The similarity between the recordings from a) and the function  $k \cdot u(t)$  from b).

Experimental conditions:

stimulus colour blue ( $460 \text{ m}\mu$ )

dark-adapted eye

stimulus duration 20 msec

dilated pupil

stimulus area  $30^\circ$  (Maxwellian view)

time-constant of the amplifier 6 sec

Finally in part c) of Fig. 6 the similarity is shown between the ERG and the appropriate  $k \cdot u(t)$ . This match turns out to be very good from  $I = 1$  up to  $I = 100$ .

If the ERG shows an  $A_s$ -wave, however, as it is the case for relative intensity  $I = 300$  we get into trouble. On the other hand we should like to know the value of  $k \cdot u(t)$  for such a composite ERG, provided that the  $B_s$ -wave continues as  $k \cdot u(t)$  under these conditions. The difficulty lies in the fact that we cannot measure the shape of an isolated  $A_s$ -wave, for it always appears in combination with a  $B_s$ -wave.

We mention two possibilities of analysing such a composite ERG on the basis of Fig. 8 and 9. Here it is assumed that the  $B_s$ -wave continues indeed as  $k \cdot u(t)$ .

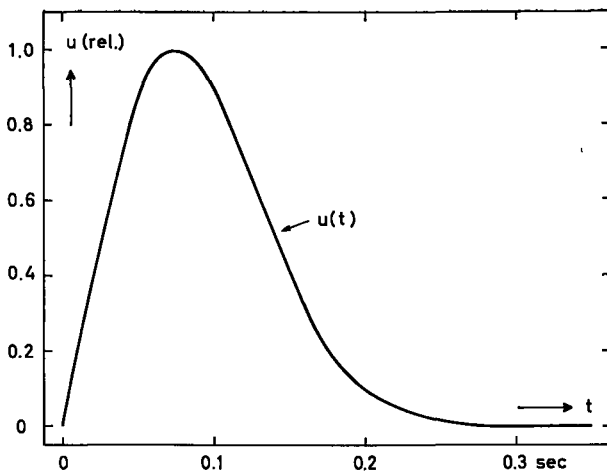


Fig. 7 - The unit-response  $u(t)$ . This unit-response represents an arbitrary  $B_s$ -wave, the amplitude of which is normalised at 1.

In Fig. 8 and 9 a composite *ERG* is thought to originate from a  $B_s$ -wave II ( $k \cdot u(t)$ ) and an  $A_s$ -wave III, by superposition of II and III with a certain delay  $\delta$ . It follows at once from these figures that various types of  $A_s$ -waves are possible, to produce a composite *ERG*. With the analysis of Fig. 8 the value of  $k$  can be found in a composite *ERG*, by measuring the height of the upward deflection from the zero-potential line. This is only exact if the  $A_s$ -wave is zero again, before the  $B_s$ -wave reaches its maximum value. The agreement between II + III and the experimentally recorded *ERG* is very good.

With the analysis of Fig. 9 the value of  $k$  can be found by measuring the height of the upward deflection from the trough of the downward deflection. This is only exact if the  $A_s$ -wave remains at a constant negative value, at least until the moment where the  $B_s$ -wave reaches its maximum value. In this situation the agreement between II + III and the experimentally recorded composite *ERG* is rather bad.

It is also possible that the shape of the  $A_s$ -wave lies between these two extreme suppositions.

In literature one usually employs an analysis of a composite *ERG*, as it is stated in Fig. 9. The main evidence for this procedure is the resemblance in this situation between an isolated  $A_s$ -wave and Granit's  $P_{III}$ -component.

We have chosen the first analysis (Fig. 8), because of the good

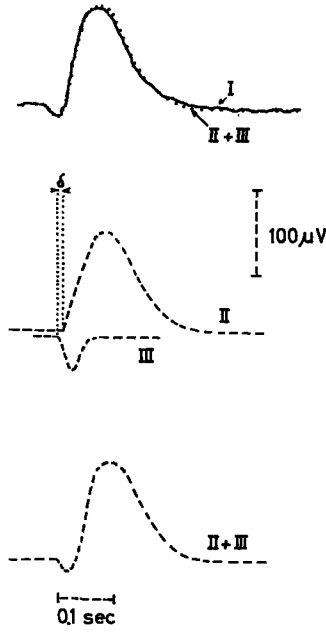


Fig. 8

- I = composite ERG, obtained with the highest stimulus intensity we employed.
- II =  $B_s$ -wave, represented by  $h.u(t)$ .
- III = possible shape of  $A_s$ -wave.

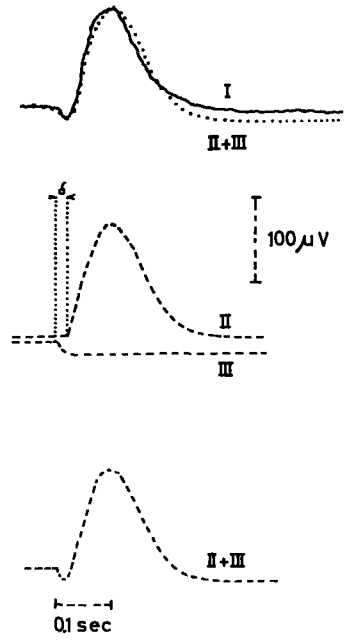


Fig. 9

- I = composite ERG (the same as in Fig. 8).
- II =  $B_s$ -wave, represented by  $h.u(t)$ .
- III = another possible shape of  $A_s$ -wave.

agreement in Fig. 8. Moreover, the calculations based on this hypothesis fitted the experimental data very well.

### C. Determination of the characteristic functions $e$ , $S$ and $g$ of the electro-retinographic system

We have already noted the fact that if the dark-adapted eye is stimulated with short blue flashes, the resulting  $B_s$ -waves can be represented by  $h.u(t)$ . This suggests that perhaps the same kind of analysis is possible as discussed in Chapter II.

Starting point of this analysis was Eq. (4), which related the input and the output of this special kind of non-linear system to each other.

$$R(T) = \int_0^T I(t) S \left[ \int_0^t I(\tau) g(t - \tau) d\tau \right] e(T - t) dt \quad (4)$$



For short stimuli, this equation reduced to Eq. (6):

$$R(T) = \{I_0 \int_0^{T_0} S[I_0 t g(0)] dt\} e(T), \quad (6)$$

where  $I_0$  is the intensity of the stimulus and  $T_0$  the duration.

A comparison of Eq. (6) and Eq. (17) shows that  $e(T)$  corresponds with the electro-retinographic unit-response  $u(t)$ , which may be any  $B_s$ -wave of normalised amplitude.

Now we look to the amplitude  $k$  of the  $B_s$ -wave as a function of the intensity  $I_0$ . In the literature  $k$  is usually plotted versus  $\log I_0$  for various durations  $T_0$ , or versus  $\log T_0$  for various intensities  $I_0$ . Because of the interchangeability of  $I_0$  and  $T_0$  for these short flashes, this is the same as  $k$  plotted versus  $\log E$ , where  $E = I_0 T_0$ .

If  $k$  is measured in  $\mu\text{V}$  and  $E$  in some arbitrary units,  $k(\log E)$  looks like an s-shaped curve. The maximum of this curve varies from subject to subject between about 100  $\mu\text{V}$  and 400  $\mu\text{V}$ . However, it appears that when these maximum values are normalised at 100%, all these curves transform into nearly the same standard curve. It looks as if there is some fundamental process underlying the shape of this standard curve, while the absolute magnitude of the response is of minor importance (it may be caused, for instance, by the internal resistance of the subject).

Three of these  $k(E)$  curves, obtained from literature, are drawn in Fig. 10 on the same scale.

The curves are shifted along the energy axis, and they can be brought into coincidence in a very good way.

The points of Schubert and Bornschein<sup>31</sup> represent the average of seven subjects, and they only noted small deviations between the various standard curves. In all these experiments the height of the  $B_s$ -wave is measured from the bottom of the  $A_s$ -wave.

However, we found that within the experimental error there is no difference between such a standard curve and a standard curve where the  $B_s$ -wave is measured from the zero-potential line. This only results in a shifting of the curve parallel to the energy axis. Thus we are allowed to compare our  $k(E)$  curve, which can be derived from Fig. 6, directly with those obtained from literature (Fig. 11).

First we want to say something now about the choice of the units in which the various quantities are measured. Therefore, we look to Eq. (17):

$$B_s\text{-wave} = k.u(t) \quad (17)$$

We suppose that  $u(t)$  always has a maximum height 1, and has no dimensions. This means that  $k$  may represent the height of the response in microvolts ( $\mu V$ ) or in percentage (%) according to the standard  $k(E)$  curve of Fig. 11.

*From now on every electrical potential that is generated by the eye under stimulation with light will be measured in %.*

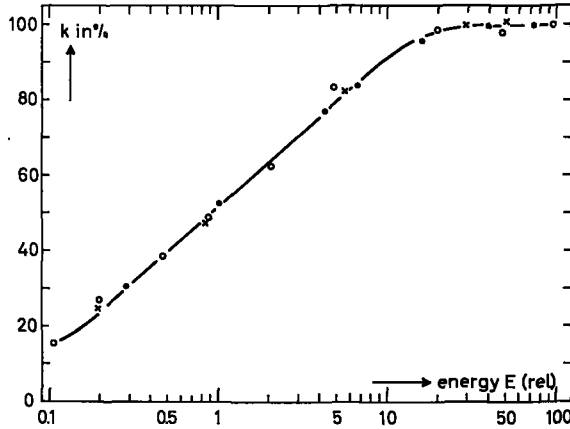


Fig. 10 - The amplitude  $k$  of the ERG response as a function of the stimulus energy  $E$  (relative units).

Maximum amplitudes normalised at 100%. In all situations the eye was dark-adapted.

- Schubert u. Bornschein<sup>81</sup>      Stimulus duration = 25msec  
    Stimulus colour = white  
    Stimulus area = 8°
- × Vukovich<sup>39</sup>                              Stimulus duration = 25msec  
    Stimulus colour = white  
    Stimulus area = 8°
- o Crampton a. Armington<sup>9</sup>          Stimulus duration = 10msec  
    Stimulus colour = blue  
    Stimulus area = 30°

The maximum height of the  $B_s$ -wave (i.e. the maximum of the standard curve) is established at 100%. The significance of this definition becomes obvious at once if we remember the constancy of the standard curve. Thus ERG's recorded under the same experimental conditions will always have equal amplitudes if measured in %.

However, the amplitudes measured in  $\mu V$  may differ strongly. Further we have to choose units in which the intensity  $I_0$  and the energy  $E$  are measured. This choice is rather arbitrary. Therefore, we define the *normalised energy unit*<sup>32</sup> in relation with a standard  $k(E)$  curve equal to the relative energy units shown on the horizontal axis of Fig. 11.

If a short stimulus evokes in the dark adapted eye a  $B_s$ -wave with an

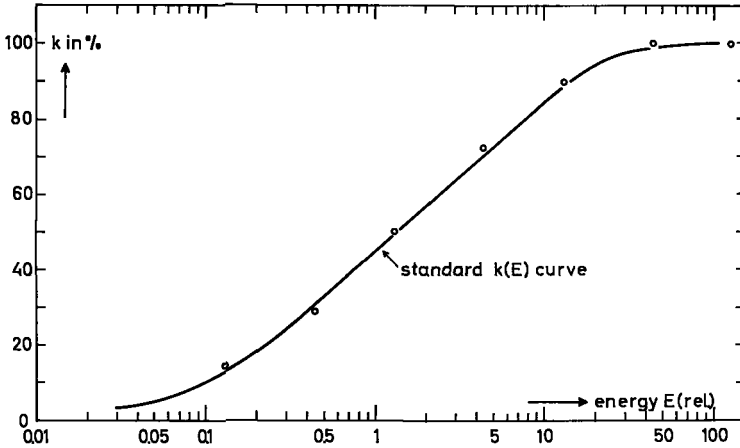


Fig. 11 - Amplitude of the *ERG* response as a function of the relative stimulus energy. Amplitude is measured from the zero-potential line.

Experimental conditions the same as in Fig. 6.

The points represent the average value of 4 measurements.

Note that this standard  $k(E)$  curve has the same shape as the curve in Fig. 10.

amplitude between 1% and 100%, the energy of the stimulus will have a value between about 0.01 and 100 normalised energy units (Fig. 11). In connection with the normalised energy unit the *normalised intensity unit*<sup>32</sup> is defined in such a way that for block-stimuli of intensity  $I_0$  and duration  $T_0$  holds:

$$I_0 \text{ (in normalised intensity units)} = \frac{E \text{ (in normalised energy units)}}{T_0 \text{ (in seconds)}}$$

Finally we note that the stimulus area has little influence on the standard  $k(E)$  curve over a big variation of areas. From measurements of Crampton and Armington<sup>9</sup> it appeared that a variation of the

testfield from about 6 degrees to 30 degrees only shifted the standard  $k(E)$  curve parallel to the horizontal axis, leaving its general shape unaltered.

Now we come to the determination of the function  $S$ . We assume that the  $k(E)$  standard curve according to Fig. 11 is known. This  $k(E)$  standard curve can be approximated very well by the following algebraic function<sup>38</sup>:

$$k(E) = 60 \log \frac{1 + 5E}{1 + 0.1E}, \quad (18)$$

where  $k$  is expressed in % and  $E$  in normalised energy units.

By using Eq. (8):

$$S[Eq(0)] = \frac{dk}{dE} = \frac{126.5}{(1 + 5E)(1 + 0.1E)}$$

$g(0)$  is an arbitrary constant and may be chosen equal to 1.

$$\text{Thus } S(E) = \frac{126.5}{(1 + 5E)(1 + 0.1E)} \quad (19)$$

The energy  $E$  in this formula is equal to:

$$E = \int_0^t I(\tau)g(t - \tau)d\tau \quad (20)$$

If the flash is block-shaped in time, with intensity  $I_0$  and short duration  $T_0$ , and it is assumed that  $g$  does not change significantly during this short time  $T_0$ , Eq. (20) transforms into:

$$E = I_0 T_0 g(0) = I_0 T_0$$

Thus only in this case  $E$  equals the real energy of the flash, but in all other situations  $E$  equals the weighted energy of the stimulus, which means that all previous intensities must be taken into account with the weighting function  $g(t)$ .

To distinguish the energy in Eq. (20) from the real energy, we will speak of the effective energy  $E_{\text{eff}}$ <sup>35</sup>, where

$$E_{\text{eff}} = \int_0^t I(\tau)g(t - \tau)d\tau$$

Finally this weighting function  $g$  has to be determined. In Chapter II we described how this can be done with the aid of double-pulses. In the electro-retinography this means we have to stimulate the eye with double-flashes. It is a well-known fact that if two short flashes of arbitrary energy are presented after each other to say, a dark-adapted eye, the second response is, in general, lower than it would be without a preceding flash (Wagman et al.<sup>40</sup>). However, there are not many quantitative data on this subject available at the moment.

In our experiments double-flashes were used, the two flashes being of equal energy (Fig. 3). An example of some experimental recordings with these double-flashes is shown in Fig. 12.

The amplitude  $k_2$  of the second response increases as the interval  $d$  between the two flashes increases, until  $k_2$  equals  $k_1$ , the amplitude of the first response. In that situation the first flash no longer influences the second response.

From Fig. 12 we can determine the ratio  $k_2/k_1$  as a function of the separation  $d$ , for three different energies per flash. All the recordings in Fig. 12 are repeated at least three times in one experimental session. The results are given in table I, where the values  $k_2/k_1$  represent the average for at least three double-flashes.

	$d$						
	0.2	0.3	0.5	0.7	1.0	1.5	
$k_2/k_1$	—	0.17	0.47	0.69	0.94	1.0	$E = 130$
$k_2/k_1$	0.29	0.45	0.63	0.89	0.98	—	$E = 13$
$k_2/k_1$	0.49	0.63	0.81	0.95	1.0	—	$E = 1.3$

Table I -  $E$  is measured in normalised energy units;  $d$  is measured in seconds

According to Eq. (11) and with  $g(0) = 1$  and  $I_0 T_0 = E$ , the ratio  $k_2/k_1$  must be equal to:

$$k_2/k_1 = \frac{k[ Eg(d) + E ] - k[ Eg(d) ]}{k(E)},$$

where  $k$  represents the standard  $k(E)$  curve.

Using  $k(E) = 60 \log \frac{1 + 5E}{1 + 0.1E}$  we obtain finally:

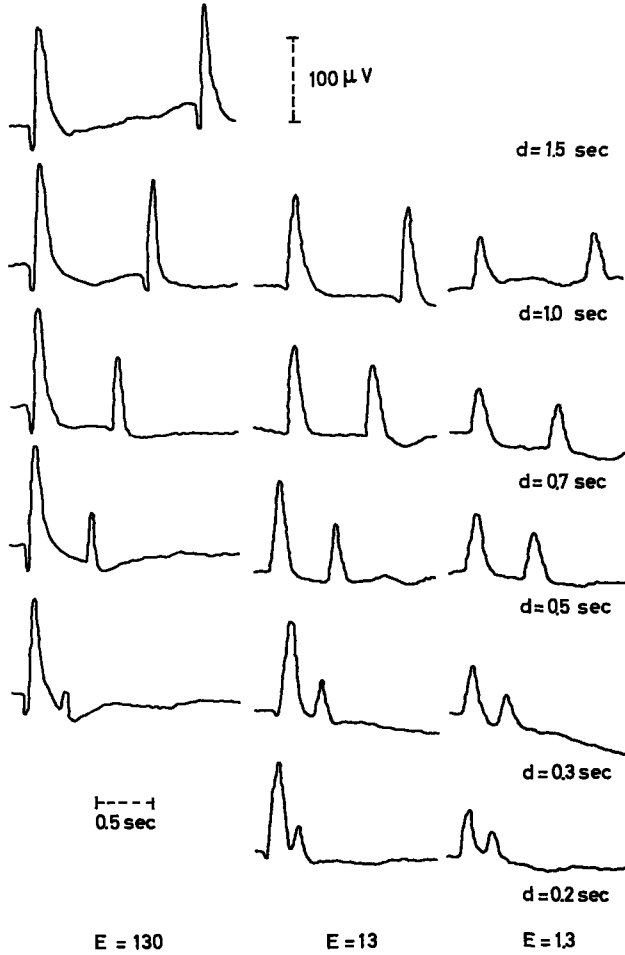


Fig. 12 - Responses to double-flashes.

In the horizontal rows the energy per flash is varied:  
 $E = 130$ ,  $E = 13$ ,  $E = 1.3$  (normalised energy units).

In the vertical columns the time  $d$  is varied:

$d = 1.5 \text{ sec}$ ,  $d = 1 \text{ sec}$ ,  $d = 0.7 \text{ sec}$ ,  $d = 0.5 \text{ sec}$ ,

$d = 0.3 \text{ sec}$ ,  $d = 0.2 \text{ sec}$ .

Other experimental conditions the same as in Fig. 6.

$$\log \left( \frac{4.9}{\frac{1}{E} + 0.1 + (5.1 + 0.5E)g(d) + 0.5Eg(d)} + 1 \right) = k_2/k_1 \log \frac{1 + 5E}{1 + 0.1E} \quad (21)$$

Eq. (21) can be solved for  $E = 130$ ,  $E = 13$ ,  $E = 1.3$ , and the specific values for  $d$  and  $k_2/k_1$  from table I. In this way the function  $g(d)$  can be calculated.

However, in this particular situation it is easier and more accurate to find the proper values for  $g(d)$  directly from the graphical representation of the standard  $k(E)$  curve in Fig. 11 by a trial-and-error method, instead of using a mathematical approximation for  $k(E)$ . The result is shown in Fig. 13, where  $g(d)$  is plotted as a function of  $d$  on a semi-logarithmic scale.

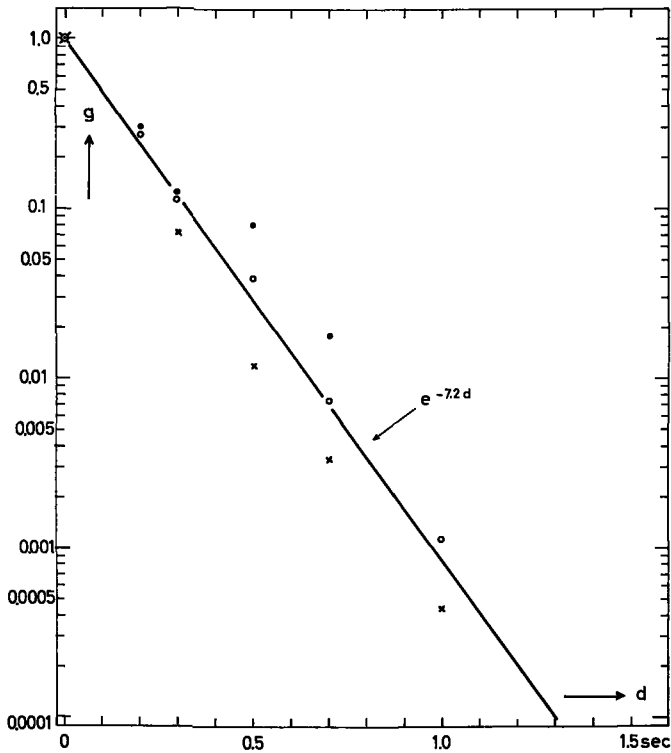


Fig. 13

- × experimentally found values of  $g$  with  $E = 130$
- o experimentally found values of  $g$  with  $E = 13$
- experimentally found values of  $g$  with  $E = 1.3$

The points show some spread, but are fairly well approximated by the straight line, in other words:

$$g(d) = e^{-7.2d} \quad (22)$$

After Eq. (5) and Eq. (20) the assumption was made that  $g$  did not change significantly during a short stimulus duration  $T_0$ , in other words

$$\int_0^{T_0} g(t - \tau) d\tau \approx T_0 g(0).$$

In order to give an idea how small  $T_0$  can be chosen, we calculated that with  $g$  defined by Eq. (22) and  $T_0 = 0.02$  sec:

$$\int_0^{T_0} g(t - \tau) d\tau = 0.0215e^{-7.2t} \text{ and } T_0 g(0) = 0.02.$$

This means that for  $0 \leq t < T_0$  an error of about  $\pm 7\%$  is made. However, in many situations this error will be much smaller. The error can be made arbitrary small by having  $T_0 \rightarrow 0$ .

The relation between input and output of the electro-retinographic system according to Eq. (4), can be written now as:

$$R(T) = \int_0^T I(t) \frac{126.5 u(T-t)}{\left(1 + 5 \int_0^t I(\tau) e^{-7.2(t-\tau)} d\tau\right) \left(1 + 0.1 \int_0^t I(\tau) e^{-7.2(t-\tau)} d\tau\right)} dt \quad (23)$$

In this equation:

$R(T)$  = electro-retinographic response.

$I(t)$  = stimulus (may be an arbitrary function of time).

$u(t)$  = response of a dark-adapted eye to a short flash; amplitude of this response normalised at 1.

Eq. (23) characterizes the electro-retinographic system under scotopic conditions, and with this equation the response to any stimulus can be calculated.



**PREDICTED AND EXPERIMENTAL RESULTS  
FOR SINGLE STIMULI**

**A. Amplitude of the B<sub>s</sub>-wave as a function of the stimulus duration for  
block-shaped stimuli**

With Eq. (23), derived in the foregoing chapter, we will calculate the amplitude of the response for various stimulus durations. We note that for short durations  $T_0$  Eq. (23) transforms into:

$$R(T) = \left[ \int_0^{T_0} \frac{126.5 I_0}{(1 + 5 I_0 t) (1 + 0.1 I_0 t)} dt \right] u(T),$$

where  $I_0$  is the intensity of the stimulus.

In other words the amplitude  $k$  of the response (in %) is equal to:

$$k = 60 \log \frac{1 + 5I_0T_0}{1 + 0.1I_0T_0}$$

This equation demonstrates the already-mentioned interchangeability of  $I_0$  and  $T_0$  for short durations. For practical purposes  $T_0$  must be shorter than 0.02 sec. In that situation the function relating the response amplitude to the stimulus duration will have the same shape as a  $k(E)$  standard curve.

For longer durations Eq. (23) can be solved numerically. We rewrite Eq. (23) as:

$$R(T) = \int_0^{T_0} H(t) u(T - t) dt, \quad (24)$$

where 
$$H(t) = \frac{126.5 I(t)}{(1 + 5 \int_0^t I(\tau) e^{-7.2(t-\tau)} d\tau) (1 + 0.1 \int_0^t I(\tau) e^{-7.2(t-\tau)} d\tau)}$$

$H(t)$  is the output of the non-linear element  $n$  and serves as the input to the linear element  $l$  (cf. Fig. 2).

For block-shaped stimuli of intensity  $I_0$  the function  $H(t)$  becomes:

$$H(t) = \frac{126.5 I_0}{[1 + 0.695 I_0 (1 - e^{-7.2t})] [1 + 0.0139 I_0 (1 - e^{-7.2t})]} \quad (25)$$

This function  $H(t)$  is calculated for  $I_0 = 2$ ,  $I_0 = 20$ ,  $I_0 = 200$  and  $I_0 = 2000$ , and represented graphically in Fig. 14. Eq. (24) can be approximated by:

$$R(T) = \underbrace{\left[ \int_0^{\Delta T_0} H(t) dt \right]}_{\Delta_1} u(T) + \underbrace{\left[ \int_{\Delta T_0}^{2\Delta T_0} H(t) dt \right]}_{\Delta_2} u(T - \Delta T_0) + \dots$$

$$+ \underbrace{\left[ \int_{(n-1)\Delta T_0}^{T_0} H(t) dt \right]}_{\Delta_n} u(T - (n-1)\Delta T_0) \quad (26)$$

The time interval  $T_0$  is divided into  $n$  equal parts  $\Delta T_0$ . The approximation in Eq. (26) is better, as  $\Delta T_0$  is chosen smaller. Here again it is sufficient if  $\Delta T_0$  is small as compared with the time constants in  $u(T)$ , for instance  $\Delta T_0 = 0.02$  sec.

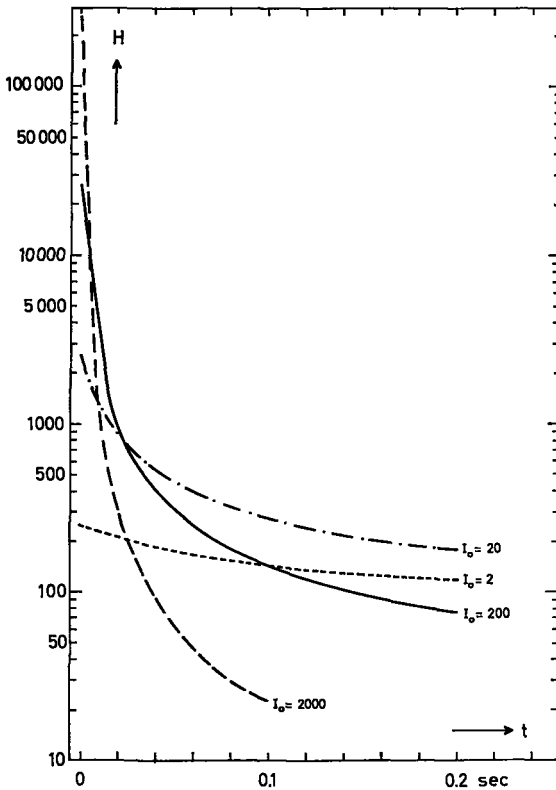


Fig. 14 - The function  $H(t)$  calculated according to Eq. (25).  $I_0$  in normalised intensity units.

The values of  $\Delta_1, \Delta_2$ , etc. for the various values of  $I_0$ , can be determined easily from the graphical representation of  $H(t)$ . These values are given in table II. For various values of  $T_0$ , which are always multiples of  $\Delta T_0$ ,  $R(T)_{\max}$  is determined from Eq. (26) as shown in table III for  $I_0 = 2$ .

These calculated values for  $R(T)_{\max}$  as a function of the stimulus duration  $T_0$  are plotted in Fig. 15 together with the experimental points.

	$\Delta_1$	$\Delta_2$	$\Delta_3$	$\Delta_4$	$\Delta_5$	$\Delta_6$	$\Delta_7$	$\Delta_8$	$\Delta_9$	$\Delta_{10}$
$I_0 = 2$	4	4	3.5	3.2	3.0	2.85	2.7	2.6	2.5	2.4
$I_0 = 20$	29	12	8.6	7.1	5.8	5.2	4.6	4.2	4.0	3.8
$I_0 = 200$	68.8	12.5	6.4	4.4	3.2	2.6	2.2	1.9	1.7	1.6
$I_0 = 2000$	98.8	1.2	-	-	-	-	-	-	-	-

Table II - Values of  $\Delta_p = \frac{p\Delta T_0}{(p-1)\Delta T_0} \int H(t)dt$

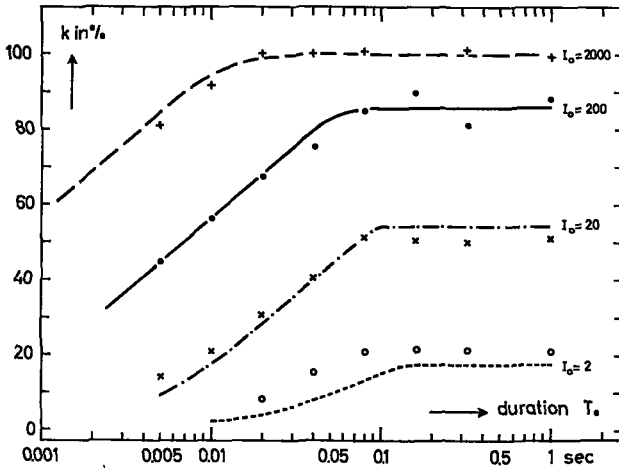


Fig. 15 - Amplitude of ERG response (in %) as a function of the stimulus duration (in seconds), for various values of the stimulus intensity (in normalised intensity units).

- o  $I_0 = 2$
  - x  $I_0 = 20$
  - $I_0 = 200$
  - +  $I_0 = 2000$
- experimental points (each point represents the average of at least 4 measurements).

The curves are calculated for the same intensities. Other experimental conditions the same as in Fig. 6.

$A_p$  from Table II.

↓ 0	0.36	0.72	0.95	0.99	0.92	0.72	0.50	0.32	0.18	0.09	0.05	0.02	0	←	$u(T)$ sampled every 0.02 sec	
4.0	0	1.44	2.88	3.80	3.96	3.68	2.88	2.00	1.28	0.72	0.36	0.20	0.08	0	$R(T)_{\max} = 3.96\%$ $T_0 = 0.02$ sec	
4.0	0	1.44	2.88	3.80	3.96	3.68	2.88	2.00	1.28	0.72	0.36	0.20	0.08	0	" = 7.76% $T_0 = 0.04$ sec	
3.5	0	1.26	2.52	3.33	3.46	3.22	2.52	2.52	1.75	1.12	0.63	0.31	0.17	0.07	0	" = 10.97% $T_0 = 0.06$ sec
3.2	0	1.15	2.30	3.04	3.17	2.95	2.30	1.60	1.02	0.58	0.29	0.16	0.06	0	" = 13.27% $T_0 = 0.08$ sec	
3.0	0	1.08	2.16	2.85	2.97	2.76	2.16	1.50	0.96	0.54	0.27	0.15	0.06	0	" = 15.22% $T_0 = 0.10$ sec	
2.85	0	1.02	2.05	2.71	2.82	2.62	2.05	1.43	0.91	0.51	0.26	-	-	-	" = 16.24% $T_0 = 0.12$ sec	
2.7	0	0.97	1.95	2.57	2.67	2.49	1.95	1.35	0.86	0.49	-	-	-	-	" = 17.14% $T_0 = 0.14$ sec	
2.6	0	0.94	1.87	2.47	2.57	2.39	1.87	1.30	0.83	-	-	-	-	-	" = 17.32% $T_0 = 0.16$ sec	
2.5	0	0.90	1.80	2.37	2.47	2.30	1.80	1.25	-	-	-	-	-	-	" = 17.32% $T_0 = 0.18$ sec	
2.4	0	0.86	1.73	2.28	2.37	2.21	1.73	-	-	-	-	-	-	-	" = 17.32% $T_0 = 0.20$ sec	

Table III - Determination of  $R(T)_{\max}$  with Eq. (26), as a function of the stimulus duration  $T_0$ .

$I_0 = 2$  normalised intensity units.

As it appears from this figure, there is a satisfactory agreement between experiment and calculation. The experimental points may be compared with similar ones obtained by Johnson and Bartlett<sup>24</sup>.

We note that there occurs a critical duration (duration above which the amplitude of the response does not increase any more). This critical duration  $T_c$  varies from about 0.02 sec for  $I_0 = 2000$  to about 0.12 sec for  $I_0 = 2$ . This can be understood in the following way:

For  $I_0 = 2000$  the  $k(T_0)$  curve, as shown in Fig. 15, is identical with the standard  $k(E)$  curve, as long as the duration remains short with respect to the time constants of the response. Consequently  $T_c$  is completely determined by the typical shape of the  $k(E)$  standard curve. For very low intensities, where a linear part may occur in the  $k(E)$  standard curve,  $T_c$  is completely determined by the shape of the unit-response  $u(t)$  (see also Johnson<sup>23</sup>). Theoretically  $T_c$  will approach a value that is equal to the duration of the unit-response, i.e. about 0.25 sec. But in practice this value cannot be measured, because of the bad signal-to-noise ratio in that situation.

For intensities  $I_0 = 2$ ,  $I_0 = 20$ ,  $I_0 = 200$ , the critical duration is determined both by the shape of the  $k(E)$  standard curve and by the shape of the unit-response  $u(t)$ , and will always have a value smaller than 0.25 sec.

There is another interesting feature that may be derived from the curves in Fig. 15. If vertical cross-sections are made through the set of curves, we find standard  $k(I_0)$  curves, valid for long stimulus durations. The result is shown in Fig. 16.

With the aid of the graphs in Fig. 16 it is possible to determine the value of  $I_0$  in normalised intensity units of any light source used in electro-retinography. The light source involved is presented in block-shaped stimuli to the dark-adapted eye of a normal subject. The stimulus duration  $T_0$  is arbitrary for  $T_0 > 0.15$  sec, but has to be known exactly for shorter durations. We only have to measure a standard  $k(I_0)$  curve now, for example, by controlling the intensity of the stimulus by neutral density filters. Comparison of such a measured curve with the calculated ones in Fig. 16, yields the value of  $I_0$  in normalised intensity units. Once more we note that the normalised unit ( $I$  or  $E$ ) depends both on the subject and the light source with accessory optics.

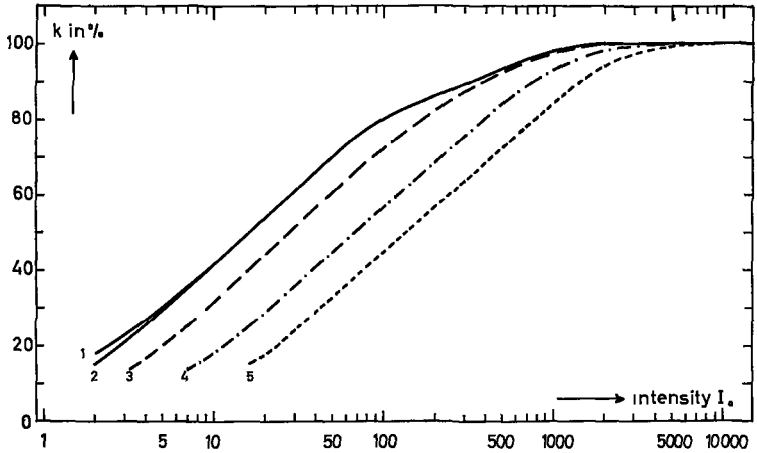


Fig. 16 - The amplitude of the response ( $k$ ) as a function of the intensity ( $I_0$ ) for various stimulus durations.

$k$  is measured in %.

$I_0$  is measured in normalised intensity units.

curve 1: stimulus duration = 0.15 sec

curve 2: stimulus duration = 0.1 sec

curve 3: stimulus duration = 0.05 sec

curve 4: stimulus duration = 0.02 sec

curve 5: stimulus duration = 0.02 sec

### B. The step-function response

In this section we will investigate the amplitude and shape of the response to positive and negative step-functions. With a positive step-function we mean a light stimulus that instantaneously changes from dark to a certain intensity  $I_0$ . A negative step-function is just the reverse. In both situations  $I_0$  is the amplitude of the step-function.

First we consider the response to a positive step-function. After a delay time the eye responds with a positive wave, which shows much resemblance to the  $B_s$ -wave to a short flash. This delay time is considered to be a transportation lag. Therefore the beginning of the response is always chosen as  $t = 0$ . Now the response to a positive step-function can be calculated with Eq. (24) and the same numerical approximations as used in Table II and III.

These calculations were carried out for four amplitudes of the step-function:  $I_0 = 7$ ,  $I_0 = 21$ ,  $I_0 = 70$  and  $I_0 = 210$  ( $I_0$  in normalised intensity units). The results are shown in Fig. 17, together with experimental recordings for the same intensities.

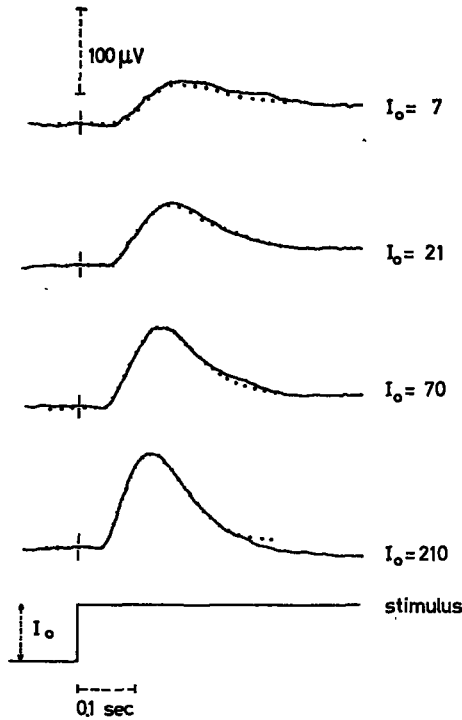


Fig. 17 - ERG recordings to a positive step-function of various intensities.  $I_0$  is measured in normalised intensity units. Other experimental conditions the same as in Fig. 6. The experimental recordings are compared with calculated responses for the same intensities (points).

The agreement is very good. In the electro-retinography this type of response is usually called the "on-effect", the response during about 0.3 sec after the beginning of the stimulus. If we look more closely at the responses in Fig. 17, we see that the response tends to a steady state where a constant dc-potential remains. This dc-potential will be maintained as long as the stimulus is on. Its amplitude can be calculated easily using Eq. (24) and (25), where  $t$  and  $T$  go to infinity. The result is:

$$\text{dc-component} = \frac{126.5 I_0}{1 + 0.7089 I_0 + 0.00965 I_0^2} \int_0^{\infty} u(T-t) dt \quad (27)$$

The term  $\int_0^{\infty} u(T-t) dt$  is a constant, which can be approximated by:

$$\int_0^{\infty} u(T-t)dt = 0.02[u(0.02) + u(0.04) + u(0.06) + u(0.08) + \dots \text{etc}]$$

$$= 0.02 (0.36 + 0.72 + 0.95 + 0.99 + 0.92 + 0.72 + 0.50 + 0.32 + 0.18 + 0.09 + 0.05 + 0.02) = 0.1165$$

Thus:

$$\text{dc-component} = \frac{14.75 I_0}{1 + 0.7089 I_0 + 0.00965 I_0^2} \quad (28)$$

From Eq. (28) we see that for low intensities the dc-component tends to zero  $\propto I_0$  and that for high intensities the dc-component tends to zero again  $\propto 1/I_0$ . Consequently there will be a medium intensity which produces a maximum dc-component.

If in Eq. (28) the intensity  $I_0$  is defined in normalised intensity units, the dc-component is found in % of the maximum obtainable  $B_s$ -wave amplitude. In Fig. 18 the calculated dc-component is plotted as a function of the intensity.

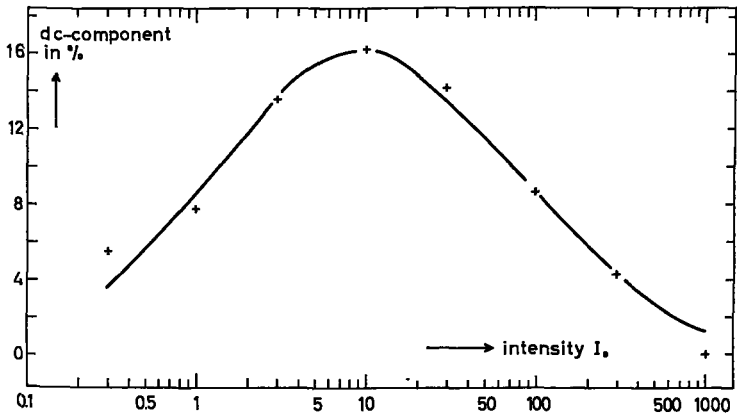


Fig. 18 - The dc-component in the response to a block-stimulus of long duration, as a function of the intensity  $I_0$  of that block-stimulus.

— calculated curve

+ measured values

The dc-component is measured in % of the maximum obtainable  $B_s$ -wave.

$I_0$  is measured in normalised intensity units.

Now we calculate the response to a negative step-function. Suppose that from  $-\infty < t < 0$  the eye has been illuminated with an intensity  $I_0$  and at  $t = 0$  this intensity falls back to zero:



The response as a function of time can be written as:

$$R(T) = \frac{126.5 I_0}{1 + 0.7089 I_0 + 0.00965 I_0^2} \int_{-\infty}^0 u(T-t) dt \quad (29)$$

Or

$$R(T) = \frac{126.5 I_0}{1 + 0.7089 I_0 + 0.00965 I_0^2} \int_T^{\infty} u(x) dx, \text{ where } x = T - t \quad (30)$$

The term  $\int_T^{\infty} u(x) dx$  is maximal for  $T = 0$  and is equal to 0 for  $T > 0.26$  sec. The exact course of  $R(T)$  can be found easily by numerical integration of  $u(x)$ . The shape of  $R(T)$  according to Eq. (30) is shown in Fig. 19.

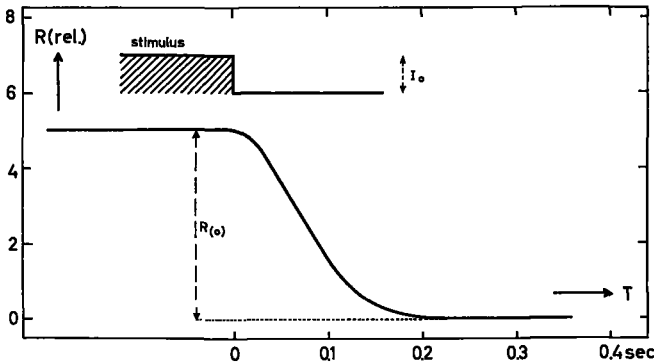


Fig. 19 - The function  $R(T)$  according to Eq. (30).

$$R(0) = \frac{14.75 I_0}{1 + 0.7089 I_0 + 0.00965 I_0^2}$$

It will be interesting now, to compare these theoretical results with experimental data. First we must find a more or less accurate way to measure the dc-component in an electro-retinographic response. It will be obvious that the elevation of the response above the zero potential line, after a sufficiently long time to allow the response to come to a steady state, will be a rather bad measure. The slow zero drift will disturb the result to a great extent.

However, if in the steady state the stimulus is switched off, we get a much more accurate method of measuring the dc-component in the

response. For according to Fig. 19 the amplitude of the response to a negative step-function of intensity  $I_0$  (end-effect) is equal to the dc-component that corresponds to that intensity  $I_0$ .

First we look at an actual response, to see if an end-effect indeed occurs, as predicted by Eq. (30) and Fig. 19. Fig. 20a and b may serve as a verification of this point.

It is found experimentally that for block-stimuli of at least 0.5 sec, the height of the end-effect does not depend on the duration of the stimulus, i.e. the steady state has been reached after about 0.5 sec.

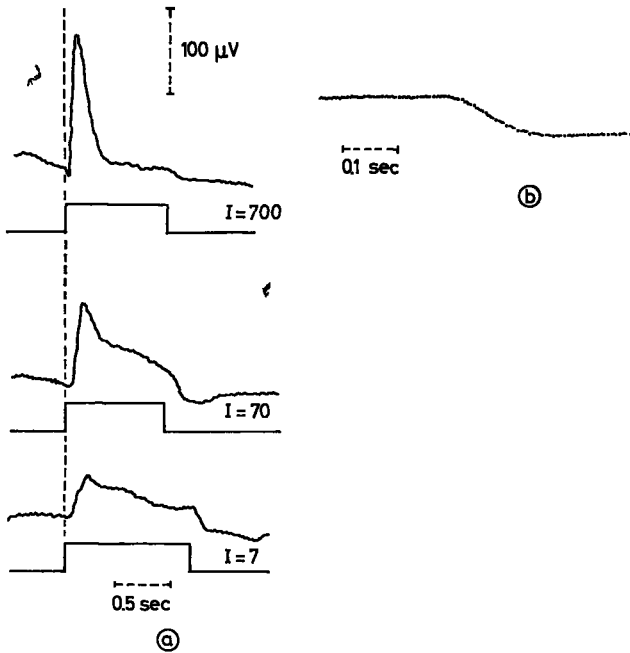


Fig. 20a - Responses to block-stimuli of long duration (about 1 sec) and of three different intensities (measured in normalised intensity units). Note the end-effect at the end of the stimulus.

b - The end-effect recorded on a large time scale.

The points indicate the calculated end-effect according to Eq. (30) and Fig. 19 and are adjusted at the appropriate scale.

The end-effect shows the same shape under these conditions, while, this shape does not depend on the intensity of the stimulus. All these facts agree with the theoretical expectations. The height of the end-

effect depends on the intensity of the stimulus, as can be seen at once from Fig. 20a.

Now this relation between the amplitude of the end-effect (i.e. the dc-potential) and stimulus intensity must satisfy Eq. (28) and Fig. 18. Therefore, we have recorded many responses to block-stimuli of long duration (0.6 sec) and various intensities. For each intensity the responses to about 10 stimuli are averaged with the average response computer (CAT), and the end-effect is measured from the result. At the same time the normalised intensity of each stimulus and the maximum obtainable  $B_s$ -wave amplitude are determined. The height of the end-effect is expressed in % of this maximum obtainable  $B_s$ -wave amplitude. The results of these measurements are plotted in Fig. 18. We see that a very good agreement exists between theory and experiment.

An investigation of the literature concerning *ERG*-work on human subjects showed that very little is known about this dc-component, as well as about the end-effect if the stimulus is turned off.

We quote from Granit's<sup>18</sup> classical work "Sensory Mechanisms of the Retina", where he discusses some scotopic *ERG*'s to long duration stimuli taken from Bernhard<sup>2</sup>: "At high intensities a small *a*-wave often develops, but there is never any off-effect. The appearance of an off-effect should always be suspected as an artefact, but the production of *a*-waves at moderate or low intensities of stimulation may be the sign of an abnormal retina, etc."

However, if the recordings of Bernhard<sup>2</sup> are studied somewhat closer, it is not impossible at all that a dc-component develops during the stimulus, even an indication of an end-effect as described in this section may be recognized at the end of the stimulus. There are several other authors who mention this dc-potential. For example: Johnson<sup>23</sup> calls it a "depletion effect" in connection with some sort of "reservoir". In the recordings presented by Bornschein and Gunkel<sup>4</sup>, the dc-potential is clearly recognizable.

Interesting are the measurements reported by Brown and Wiesel<sup>7</sup>. These authors analysed the intra-retinal electro-retinogram in the intact cat eye. Using stimuli of a duration of 0.8 sec and several intensities, they found a dc-potential and off-effect at the end of the stimulus, that resembles very much the analogous phenomena in the human *ERG*, as described in this section.

We may conclude by stating that although there are several qualitative indications about this dc-potential in the literature, a quantitative

treatment of this subject could not be found. Perhaps the material presented in this section may fill up a gap regarding this point.

### C. The ramp-function response

With the characterization of the electro-retinographic system, as outlined in the foregoing sections, it is, of course, possible to calculate the response to any stimulus, provided that the intensity is not too high. As another example of this procedure, we will calculate the response to a ramp-function. Thus the stimulus can be represented by:

$$I(t) = aI_0t \quad (31)$$

According to Eq. (24) the ERG reponse  $R(T)$  can be written as:

$$R(T) = \int_0^T H(t)u(T-t)dt, \quad (32)$$

where

$$H(t) = \frac{126.5 aI_0t}{[1 + 5aI_0 \int_0^t \tau e^{-7.2(t-\tau)} d\tau] [1 + 0.1aI_0 \int_0^t \tau e^{-7.2(t-\tau)} d\tau]} \quad (33)$$

By solving the integrals in Eq. (33) the function  $H(t)$  transforms into:

$$H(t) = \frac{126.5 aI_0t}{\left[1 + \frac{5aI_0}{7.2} \left\{t - 0.139(1 - e^{-7.2t})\right\}\right] \left[1 + \frac{0.1aI_0}{7.2} \left\{t - 0.139(1 - e^{-7.2t})\right\}\right]} \quad (34)$$

From Eq. (34) it is clear that the ramp-function response always approaches zero as  $t$  (and  $T$ ) go to infinity.

We restrict ourselves to 4 ramp-functions of different slopes, and all of a duration of 0.4 sec, as shown in Fig. 21.

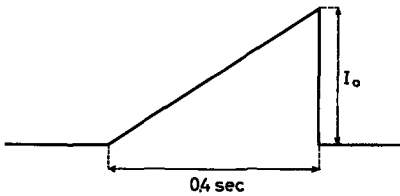


Fig. 21 - Ramp-function stimulus.

- 1)  $I(t) = 25t$  ( $I_0 = 10$ )
  - 2)  $I(t) = 75t$  ( $I_0 = 30$ )
  - 3)  $I(t) = 250t$  ( $I_0 = 100$ )
  - 4)  $I(t) = 750t$  ( $I_0 = 300$ )
- $I_0$  in normalised intensity units.

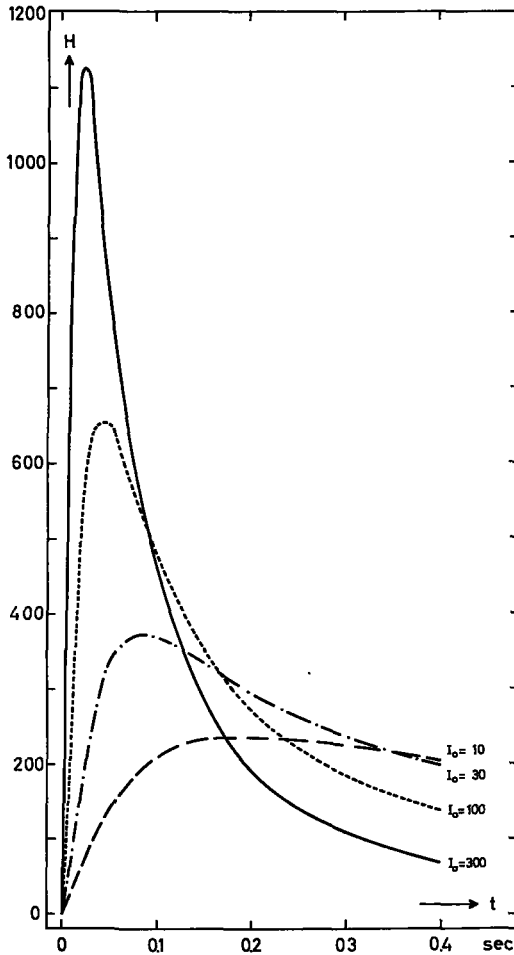


Fig. 22 - The function  $H(t)$  according to Eq. (34) for 4 different slopes of the ramp-function  $I(t) = \alpha I_0 t$ .  $I_0$  is expressed in normalised intensity units.

The function  $H(t)$  is calculated for these 4 values of  $\alpha I_0$  according to Eq. (34). The result is shown in Fig. 22.

In exactly the same way as demonstrated in the previous section for the step-function response, the integral in Eq. (32) is integrated numerically, and the 4 ramp-function responses  $R(T)$  are shown in Fig. 23, together with experimental recordings for the same intensities. The agreement between calculation and experiment is not too bad, both the calculated and measured responses show the same trend.

We note that small deviations of the stimulus from a ramp-function, especially at the beginning, may affect the results to a relatively large extent. Furthermore, it is difficult to avoid a slow zero drift during these long recordings, which take about 0.8 sec. The recordings in Fig. 23 are nice samples, but many had to be rejected for the reasons just mentioned.

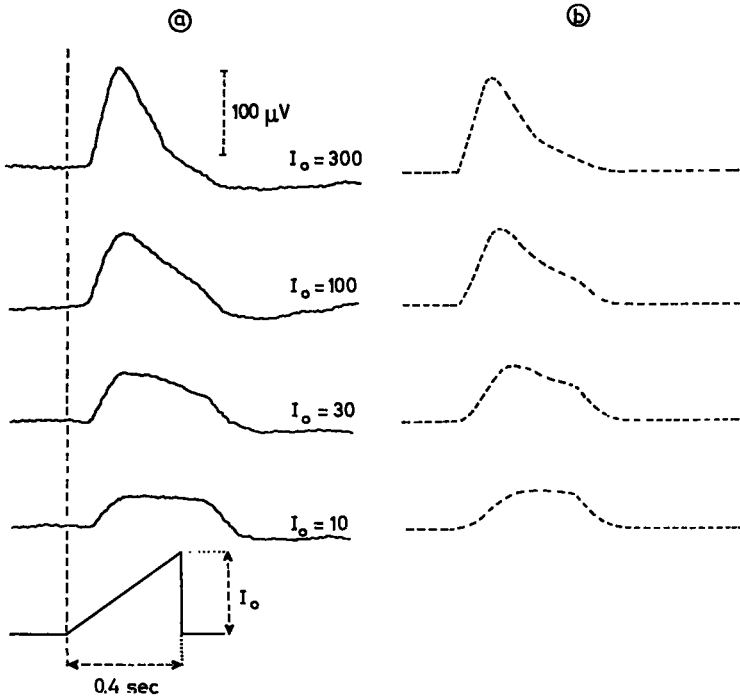


Fig. 23a - Experimental ramp-function responses. Duration of the ramp-function 0.4 sec. Other experimental conditions the same as in Fig. 6.  $I_0$  in normalised intensity units.

b - Calculated responses for the same intensities.

The importance of the rise-time of the stimulus has been pointed out already by Bornschein and Gunkel<sup>4</sup>. Their results should be predictable if analysed by an analogous procedure as outlined in this section. Therefore, the  $h(E)$  standard curve, the weighting function  $g(t)$  and the unit-response  $u(t)$  of the subject involved have to be known.

#### D. Analysis of an arbitrary response

An interesting aspect of the theory discussed in the previous sections, is the fact that it is completely reversible. This means that if an arbitrary response is given in % of the maximum obtainable  $B_s$ -wave amplitude, it is possible to calculate the shape and the intensity of the stimulus necessary to evoke that response. Only the three fundamental functions of the subject involved have to be known, i.e. the  $k(E)$  standard curve, the weighting function  $g(t)$  and the unit-response  $u(t)$ . However, this procedure is rather inaccurate. To go from the response to the stimulus, a more or less inverse logarithmic operation is performed. In other words, small errors in the response result in large errors in the stimulus.

#### E. Conclusion

In the foregoing sections we have investigated the relation between a single light stimulus and the resulting *ERG* response under certain restricted conditions. These investigations were done on one normal subject.

It appeared to be possible to describe the relation stimulus  $\rightarrow$  *ERG* by three fundamental functions:

- a. The unit-response  $u(t)$ .
- b. The  $k(E)$  standard curve.
- c. The weighting function  $g(t)$ .

a) The unit-response  $u(t)$ . The shape of this unit-response is determined by the response of the dark-adapted eye to a short flash of light. We found that the  $u(t)$  of one subject did not vary over a period of at least three years. To see if the same  $u(t)$  holds for other normal subjects, we have looked in the literature for  $B_s$ -wave recordings which are obtained from dark-adapted eyes with short flashes, and are reproduced on a sufficiently large time-scale. Some of these responses are represented in Fig. 24. They are compared with the function  $u(t)$  from Fig. 7. The amplitude and the time-scale of our  $u(t)$  are transformed at appropriate values.

It follows from Fig. 24 that the agreement between the responses and  $u(t)$  is rather good. Thus  $u(t)$  does not seem to vary much from subject to subject if only normal subjects are considered. It may be interesting to see if  $u(t)$  is altered in pathological situations.

b) The  $k(E)$  standard curve. We mentioned already that this curve

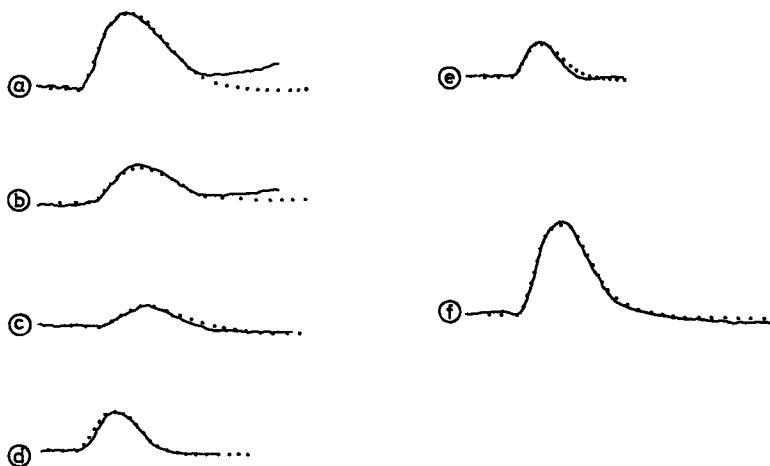


Fig. 24 - Recordings of the  $B_s$ -wave, derived from literature, and compared with our unit-response  $u(t)$  (points).

- |  |  |
|--|--|
| a)b)c) Riggs and Johnson <sup>30</sup><br>Stimulus duration: 40 msec<br>Stimulus colour: white<br>Dark-adapted eye           | e) Schubert und Bornschein <sup>31</sup><br>Stimulus duration: 25 msec<br>Stimulus colour: blue<br>Dark-adapted eye (partly) |
| d) Bornschein und Vukovich <sup>5</sup><br>Stimulus duration: 25 msec<br>Stimulus colour: white<br>Dark-adapted eye (partly) | f) Own measurements<br>Stimulus duration: 20 msec<br>Stimulus colour: blue<br>Dark-adapted eye                               |

shows a very constant shape, in so far as normal subjects are involved. Again it remains to be seen whether this also holds true in pathological situations.

c) The weighting function  $g(t)$ . About this function little is known. The experimental data presented in the literature are always insufficient to construct this weighting function. More research at this point, both in normal and pathological situations may be very important.

Finally we will make some remarks on the determination of these three fundamental functions.

As to the unit-response  $u(t)$  and the  $h(E)$  standard curve, the procedure is straightforward. We may obtain  $u(t)$  by averaging many  $B_s$ -waves, evoked under identical conditions, such as a good dark-adaptation, short stimulus duration, constant stimulus energy, dilated pupil, and so on. The  $h(E)$  standard curve can be found if, under the same experi-



mental conditions as mentioned above, the stimulus energy is varied. However, there are several methods to determine the weighting function  $g(t)$ . For instance, this function can be found from the  $k(E)$  standard curve and a double-flash experiment in which the ratio  $k_2/k_1$  is determined for one flash energy and various intervals between the two flashes.

Another possibility is to choose an indirect method. If the standard  $k(E)$  curve and the unit-response  $u(t)$  are known, and if, moreover, the response to a given long duration stimulus is measured, the weighting function can be found by analysing this response.

PREDICTED AND EXPERIMENTAL RESULTS  
FOR REPETITIVE STIMULI

A. Short flashes with low repetition frequencies

Suppose the stimulus to be a series of flashes with repetition frequency  $\nu$  as shown in Fig. 25.

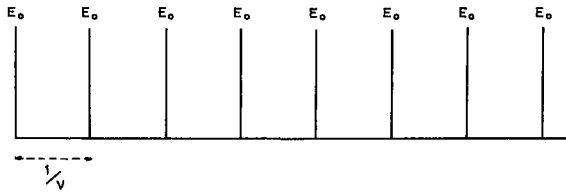


Fig. 25 - Series of flashes (duration  $T_0$ , energy per flash  $E_0$ , intensity  $I_0$ ) with repetition frequency  $\nu$  cps.

$T_0 \ll 1/\nu$       Stimulus colour blue.  
Dilated pupil.  
Dark-adapted eye at the beginning of a stimulus.

The duration  $T_0$  of each flash is thought to be short as compared with the interval between two flashes and with the time constants in the resulting response. As the repetition frequency in our experiments will never exceed 20 cps, for practical purposes  $T_0$  must be shorter as 0.01 sec. The flashes are of equal energy  $E_0$ , the interval between the flashes is  $1/\nu$  sec. In the *ERG* response two events can be distinguished: a transient and some sort of forced oscillation, the main frequency of which will be equal to the repetition frequency of the flash. After a sufficiently long time to allow the transient to damp out, only the forced oscillation remains and the system has come to an equilibrium. Now we ask for the response, after this steady state has been reached. Again our starting point is Eq. (24):

$$R(T) = \int_0^T H(t)u(T-t)dt, \text{ with} \tag{24}$$

$$H(t) = \frac{126.5 I(t)}{(1 + 5 \int_0^t I(\tau) e^{-7.2(t-\tau)} d\tau) (1 + 0.1 \int_0^t I(\tau) e^{-7.2(t-\tau)} d\tau)}$$

Here  $I(\tau)$  is represented in Fig. 25. We calculate the value of  $H(t)$  at  $t = n/\nu$ , where  $n$  is some arbitrary positive integer. Then we find for  $H(n/\nu)$ :

$$H(n/\nu) = \frac{126.5 I_0}{[1 + 5E_0(e^{-7.2/\nu} + \dots + e^{-7.2n/\nu})][1 + 0.1E_0(e^{-7.2/\nu} + \dots + e^{-7.2n/\nu})]} \quad (35)$$

If  $n$  is large, i.e. after a sufficiently large number of flashes to insure that a steady state has been reached, Eq. (35) can be approximated by:

$$H(n/\nu) = \frac{126.5 I_0}{\left[1 + 5E_0 \frac{e^{-7.2/\nu}}{1 - e^{-7.2/\nu}}\right] \left[1 + 0.1E_0 \frac{e^{-7.2/\nu}}{1 - e^{-7.2/\nu}}\right]}$$

This means that in the steady state the linear part of the system, characterized by its unit-response  $u(t)$ , is stimulated with short impulses of equal energy:

$$\int_{n/\nu}^{n/\nu+T_0} H(t) dt = \int_0^{T_0} \frac{126.5 I_0 dx}{\left[1 + 5E_0 \frac{e^{-7.2/\nu}}{1 - e^{-7.2/\nu}} + 5I_0 x\right] \left[1 + 0.1E_0 \frac{e^{-7.2/\nu}}{1 - e^{-7.2/\nu}} + 0.1I_0 x\right]}$$

Working out the integral in this equation results in:

$$\int_{n/\nu}^{n/\nu+T_0} H(t) dt = 60 \log \frac{1 + 5E_0 \frac{e^{-7.2/\nu}}{1 - e^{-7.2/\nu}} + 5I_0 T_0}{1 + 0.1E_0 \frac{e^{-7.2/\nu}}{1 - e^{-7.2/\nu}} + 0.1I_0 T_0} - 60 \log \frac{1 + 5E_0 \frac{e^{-7.2/\nu}}{1 - e^{-7.2/\nu}}}{1 + 0.1E_0 \frac{e^{-7.2/\nu}}{1 - e^{-7.2/\nu}}} \quad (36)$$

According to Eq. (24) the steady state response  $R_{ss}$  of the electroretinographic system can be written as:

$$R_{ss} = \left\{ \int_{n/\nu}^{n/\nu + T_0} H(t) dt \right\} \underbrace{\left\{ \dots + u(t + \frac{1}{\nu}) + u(t) + u(t - \frac{1}{\nu}) + u(t - \frac{2}{\nu}) + \dots \right\}}_{U(\nu, t)} \quad (37)$$

The function  $U(\nu, t)$  in Eq. (37) means that the unit-responses  $u(t)$  are superimposed with intervals  $1/\nu$ , until a steady state has been reached. In this steady state  $U(\nu, t)$  consists of a dc-component with a variation superimposed on it. If the repetition frequency  $\nu$  increases, while the energy per flash remains at a constant value, this variation decreases in amplitude and the dc-component increases. As we restrict ourselves in this section to low repetition frequencies ( $\nu < 20$  cps), we are only interested in the variation, this being the most conspicuous part of the response.

Now we calculate the amplitude of the variation in  $U(\nu, t)$  for the steady state condition. This is performed by a numerical superposition of the unit-responses  $u(t)$ . We show an example of the procedure for  $\nu = 8.34$  cps in Table IV. In an analogous way the amplitude of the variation in  $U(\nu, t)$  is calculated for other repetition frequencies. The result is presented in Fig. 26.

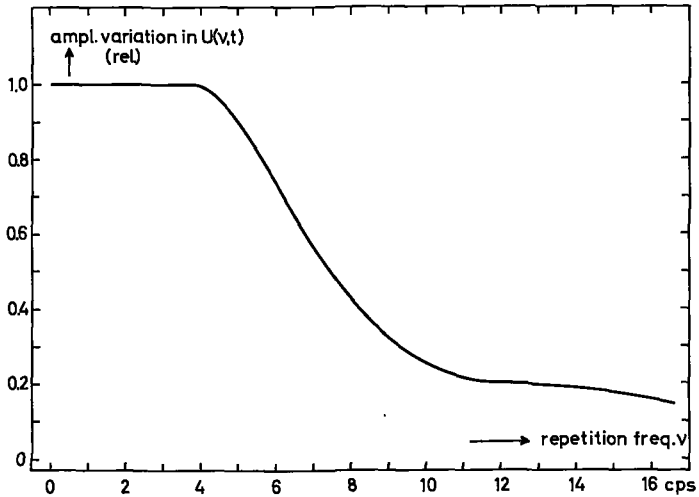


Fig. 26 - Amplitude of the variation in  $U(\nu, t)$  as a function of the repetition frequency  $\nu$ , in the steady state.  $U(\nu, t)$  originates from a linear superposition of unit-responses  $u(t)$ , occurring with intervals  $1/\nu$  sec.

0.18	0.09	0.05	0.02	0						←		
0.95	0.99	0.92	0.72	0.50	0.32	0.18	0.09	0.05	0.02	0	←	$u(t)$ sampled
			0	0.36	0.72	0.95	0.99	0.92	0.72	0.50	←	every 0.02 sec
									0	0.36	←	
(+)												
1.13	1.08	0.97	0.74	0.86	1.04	1.13	1.08	0.97	0.74	0.86	←	$U(v,t)$ in the steady state

Table IV - A superposition of unit-responses  $u(t)$ . The interval between the unit-responses is equal to  $\frac{1}{8.34} = 120$  msec. The amplitude of the variation in  $U(v,t)$  in the steady state is seen to be  $1.13 - 0.74 = 0.39$ .

With these data we are able now to calculate the amplitude of the varying part in the *ERG* response as a function of the energy and repetition frequency of the flashes. This has been done for two energies per flash,  $E_0 = 3.3$  and  $E_0 = 0.33$  respectively ( $E_0$  measured in normalised energy units).

Some significant data concerning these two energies per flash are shown in Table V. The amplitude of the variation in the response can be found from Table V as:

$$\text{amplitude variation} = \left\{ \int_{n/\nu}^{n/\nu+T_0} H(t) dt \right\} \left\{ \text{variation in } U(v,t) \right\} \quad (38)$$

		$\nu$							
		1	2	3	4	6	8	10	
$E_0 = 3.3$	$\int_{n/\nu}^{n/\nu+T_0} H(t) dt$	67.2	57.6	44.4	34.0	22.3	15.9	11.8	
	variation in $U(v,t)$	1	1	1	0.99	0.735	0.42	0.25	
$E_0 = 0.33$	$\int_{n/\nu}^{n/\nu+T_0} H(t) dt$	24.5	23.8	22.2	20.1	16.8	14.1	12.0	
	variation in $U(v,t)$	1	1	1	0.99	0.735	0.42	0.25	

Table V - Calculated values for  $\int_{n/\nu}^{n/\nu+T_0} H(t) dt$ , according to Eq. (36), and the variation in  $U(v,t)$  for two energies and various repetition frequencies.

The result is plotted in Fig. 28 (curves). The experimental recordings are shown in Fig. 27a and b.

From these experimental recordings the amplitude of the variation in the response can be determined by averaging over a sufficient long

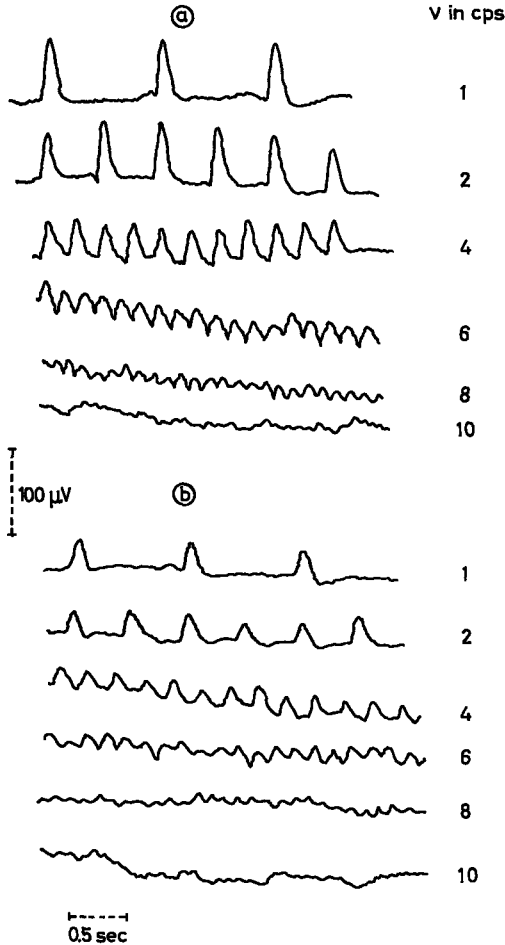


Fig. 27 - ERG response to series of flashes of various repetition frequencies after a steady state has been reached.

a) Energy per flash: 3.3 normalised energy units.

b) Energy per flash: 0.33 normalised energy units.

Experimental conditions:

Dark-adapted eye.

Stimulus colour blue.

Flash duration 100  $\mu$ sec.

Dilated pupil.

The time constant of the recording equipment is 6 sec.

period of time (for the lower repetition frequencies this time interval was longer than represented in Fig. 27). These experimental data are also plotted in Fig. 28 (points).

As can be seen from Fig. 28, the agreement between the experimental points and the calculated curves is good.

In literature the data about this subject are usually restricted to

measurements of the flicker fusion frequency. This flicker fusion frequency is defined as the highest repetition frequency of the flash, at which a ripple (of the same frequency) can be distinguished in the response. Clearly this is a rather unfortunate definition. The flicker fusion frequency depends both on the characteristics of the recording apparatus (e.g. the signal-to-noise ratio), and the ability of the investigator to recognize a response in the irregular pattern of the recording.

Henkes, v. d. Tweel and Denier v. d. Gon<sup>20</sup> improved the signal-to-noise ratio by a selective amplification of the electro-retinogram, but still the difficulty remains to define an objective flicker fusion frequency.

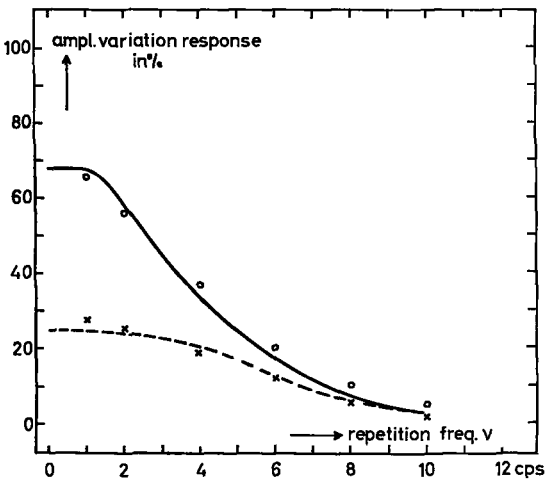


Fig. 28 - Amplitude of response plotted versus repetition frequency  $\nu$ , for two energies per flash.

○ experimental points for  $E_0 = 3.3$   
 × experimental points for  $E_0 = 0.33$   
 The curves are calculated for the same energies.

From the data presented in this section it is possible to calculate a flicker fusion frequency as soon as a criterion for a just detectable response has been established. We consider the following criteria:

- a. An amplitude at 10% level is just detectable.
- b. An amplitude at 5% level is just detectable.
- c. An amplitude at 1% level is just detectable.
- d. An amplitude at  $\frac{1}{2}\%$  level is just detectable.

These amplitudes in % are related to the maximum obtained  $B_s$ -wave (in the dark-adapted eye), which is put at 100%.

By an extension of the number of theoretical curves to more values of energy per flash, thereby relating the amplitude of the response to the repetition frequency as presented in Fig. 28, and by calculating each curve for higher repetition frequencies, it is possible to determine the flicker fusion frequencies that correspond to the various criteria of a just detectable response. The result of this calculation is shown in Fig. 29.

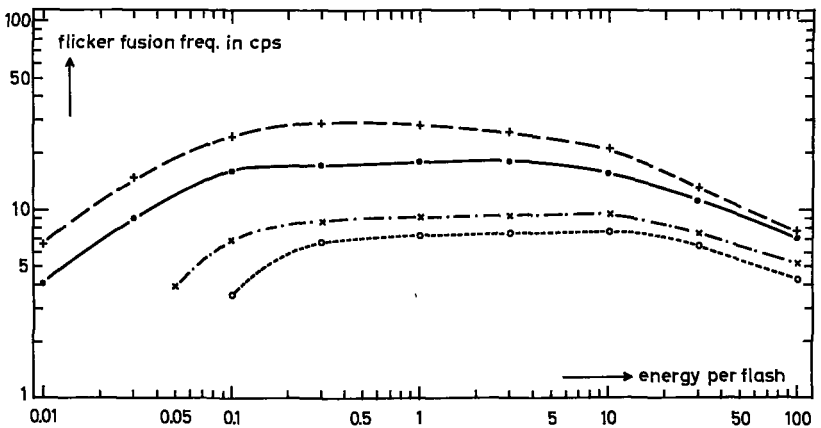


Fig. 29 - The flicker fusion frequency calculated as a function of the energy per flash, for various criteria of a just detectable response.

- 10% criterion
- × 5% criterion
- 1% criterion
- + 0.5% criterion

Energy per flash is measured in normalised energy units.

Now we want to compare these results with experimental data obtained from literature. Therefore, we have chosen the investigations of Goodman and Iser<sup>15</sup>. Their experimental conditions are much the same as the assumptions upon which our theoretical considerations are based.

These authors report experiments in which the flicker fusion frequency is measured as a function of the stimulus intensity. Two cases are of special interest: the flicker fusion frequency of a normal dark-adapted subject and of a totally colour blind dark-adapted subject.



The responses of a dark-adapted, totally colour blind subject are thought to have a completely scotopic origin (Vukovich<sup>39</sup>). Therefore the most conspicuous part of the response will be the scotopic  $B_s$ -wave and the flicker fusion frequency may be compared directly with one of the calculated curves in Fig. 29. It appeared that the curve based on the 1% criterion yielded the best fit (Fig. 30). As 1% usually corresponds with about  $2 \mu V$ , this seems a very reasonable value. We make some remarks in connection with Fig. 30. Our theoretical curve has been calculated for normalised energy values of the flash. From the experimental data of Goodman and Iser<sup>15</sup> we could not

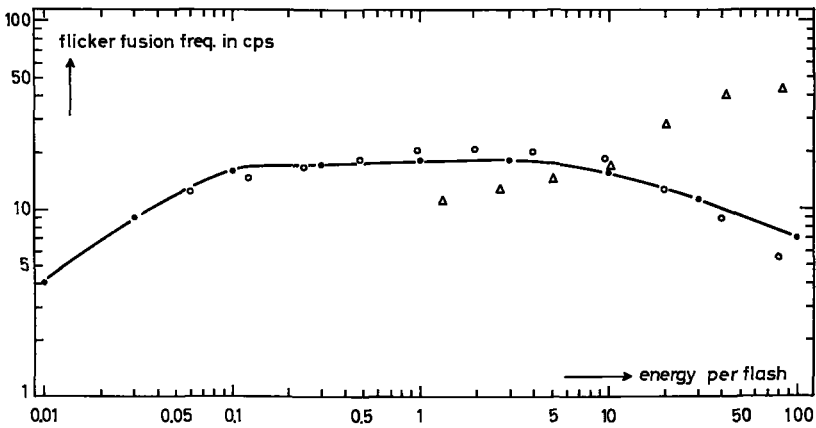


Fig. 30 - - - - Theoretical flicker fusion frequency based on the 1% criterion, together with experimental points, derived from literature. Energy per flash is measured in normalised energy units.

- O Totally colour blind subject (Goodman and Iser<sup>15</sup>).
- △ Normal subject (Goodman and Iser<sup>15</sup>).

Both subjects were dark-adapted. Stimulus colour white.

determine how to calibrate their scale of arbitrary units on our scale of normalised units. Hence, the experimental points may be shifted arbitrarily in horizontal direction.

Moreover, we do not know how the three fundamental functions describing the system: stimulus  $\rightarrow$  ERG (cf. Chapter IV), would appear for a totally colour blind subject. They probably do not, however, differ very much from the "normal" fundamental functions, which are based on the scotopic behaviour of the eye.

After these restrictions, the striking features in Fig. 30 are the following.

The experimental points for the dark-adapted, totally colour blind subject show the same course as the calculated curve, as was to be expected, since our calculations are also based chiefly upon the scotopic functions of the eye.

The experimental points for the dark-adapted, normal subject show a completely different course, in which two branches may be distinguished. The lower branch is attributed to the scotopic system, while the other one is thought to have a photopic origin. Consequently the lower branch must be compared with our theoretical curve. Our own experience was that between energies per flash of 10 and 100 normalised energy units, the response of the eye lost its scotopic character if a white stimulus was used. In that situation the fusion was determined by  $A_p$ - and  $B_p$ -waves. This yields a higher flicker fusion frequency because of the fast character of the photopic waves.

Concluding this section, we mention a phenomenon in electro-retinography often described as the "nonflickering" period (Goodman and Iser<sup>15</sup>). This means that after an initial on-effect at the beginning of a series of flashes, there may occur a period in which the amplitude of the varying part of the response is lower, as in the steady state, or sometimes fails completely.

We found, with a trained subject, that this effect is difficult to reproduce, and that often a nonflickering period did not occur at all. As a matter of fact, such a nonflickering period can not be described by a theory as developed in this thesis.

### B. Short flashes with high repetition frequencies

In section A we mentioned that for low repetition frequencies ( $\nu < 20$  cps) the varying part in the steady state response is the most conspicuous part. This variation decreases as the repetition frequency increases, and for  $\nu \approx 20$  cps the variation is hardly detectable any more.

As the repetition frequency increases further, the dc-component in the steady state response becomes important. If  $\nu > 20$  cps the duration of a cycle is smaller than 0.05 sec. This 0.05 sec is already rather small as compared with the time constants of  $u(t)$ , and consequently the intensity  $I_0$  and the duration  $T_0$  of the flash are interchangeable

within a cycle. This means that the two stimuli shown in Fig. 31 will cause the same dc-component. In other words, the dc-component is a function of the average intensity only.

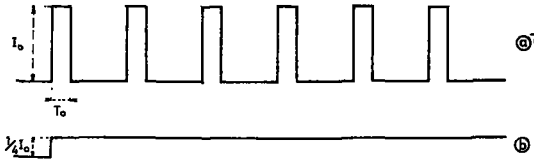


Fig. 31a - Series of flashes with repetition frequency  $\nu = 25$  cps.

$I_0$  = intensity of the flash.

$T_0$  = duration of the flash ( $T_0 = 0.01$  sec).

b - Block-shaped stimulus of intensity  $1/4 I_0$ .

The responses to these two stimuli will have the same dc-potential.

With regard to the foregoing the dc-component can be calculated most easily by treating the series of flashes as a continuous stimulus of appropriate intensity and by applying the methods developed in Chapter IV, Sec. B.

Experiments done with series of flashes of these high repetition frequencies showed exactly the same results as experiments done with block-stimuli of long duration.

### C. Sinusoidal stimulation

If the electro-retinographic system is stimulated with a time varying intensity equal to  $I(t) = I_0(1 + \rho \sin \omega t)$ , then according to Eq. (12a) and (b) the response is given by:

$$R(T) = \int_0^T H(t) u(T-t) dt \quad (39a)$$

$$H(t) = \frac{126.5 I_0 (1 + \rho \sin \omega t)}{\{1 + 5I_0 \int_0^t (1 + \rho \sin \omega \tau) e^{-7.2(t-\tau)} d\tau\} \{1 + 0.1I_0 \int_0^t (1 + \rho \sin \omega \tau) e^{-7.2(t-\tau)} d\tau\}} \quad (39b)$$

Evaluating of the integrals in Eq. (39b) results in:

$$H(t) = \frac{126.5 I_0 (1 + \rho \sin \omega t)}{\left[ 1 + \frac{5I_0}{7.2} (1 - e^{-7.2t}) + \frac{5\rho I_0}{\omega^2 + 7.2^2} (7.2 \sin \omega t - \omega \cos \omega t + \omega e^{-7.2t}) \right]} \times$$

$$\times \frac{1}{\left[ 1 + \frac{0.1I_0}{7.2} (1 - e^{-7.2t}) + \frac{0.1\rho I_0}{\omega^2 + 7.2^2} (7.2 \sin \omega t - \omega \cos \omega t + \omega e^{-7.2t}) \right]} \quad (40)$$

As we are only interested in the response of the system after a sufficiently long enough time such that a steady state has been reached, Eq. (40) transforms into:

$$H(t) = \frac{126.5 I_0 (1 + \rho \sin \omega t)}{\left[ 1 + \frac{5I_0}{7.2} + \frac{5\rho I_0}{\omega^2 + 7.2^2} (7.2 \sin \omega t - \omega \cos \omega t) \right]} \times$$

$$\times \frac{1}{\left[ 1 + \frac{0.1I_0}{7.2} + \frac{0.1\rho I_0}{\omega^2 + 7.2^2} (7.2 \sin \omega t - \omega \cos \omega t) \right]} \quad (41)$$

Now we first try to find the solution of Eq. (39a) if  $H(t) = A \sin \omega t$ . As mentioned already in Chapter II, Sec. C, Eq. (39a) describes a linear system stimulated with the time function  $H(t)$ . Such a linear system is characterized either in the time-domain, for example, by its impulse response  $u(t)$ , or in the frequency-domain by the amplitude-frequency and phase-frequency characteristics, i.e. the complex frequency function  $G(j\omega)$ . The impulse response and the complex frequency function form a Fourier transform pair:

$$G(j\omega) = \int_0^{\infty} u(t) e^{-j\omega t} dt, \text{ with} \quad u(t) = 0 \text{ for } t \leq 0 \quad (42)$$

To evaluate the integral in Eq. (42) we apply Guillemin's impulse method as outlined by Truxal<sup>36</sup>. This procedure goes as follows:

In Fig. 32a the original impulse response  $u(t)$  is shown. This function is differentiated with respect to  $t$  (numerically or graphically). Next the function  $u'(t)$  is approximated by broken lines (Fig. 32b). In fact, this step means that  $u(t)$  is approximated by curves of the second degree. After this the broken-line approximation of  $u'(t)$  is differentiated another two times with respect to  $t$ , in order to get a set of impulses

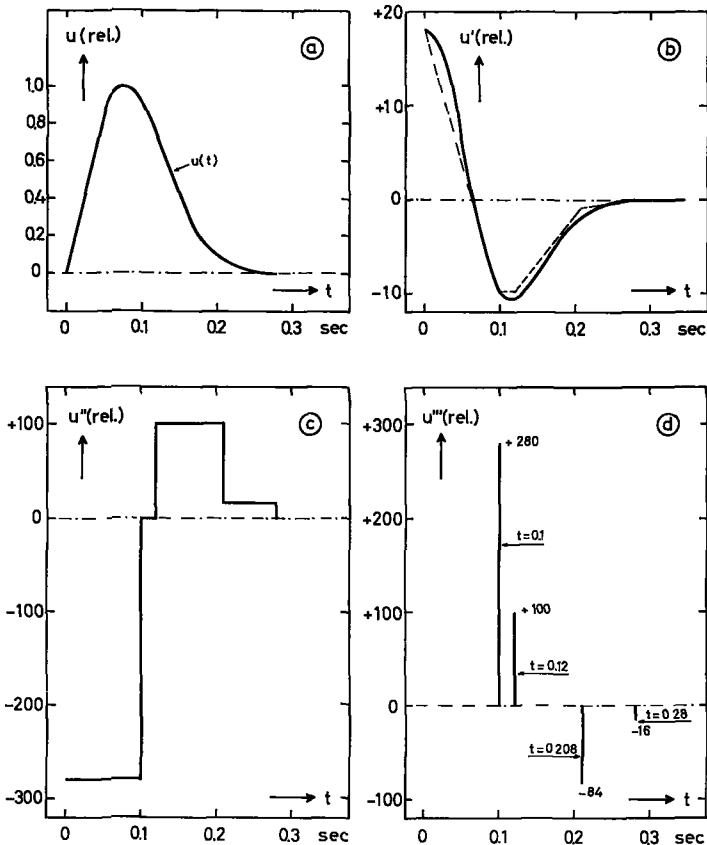


Fig. 32a - The impulse response  $u(t)$ .  
 b - The first derivative of  $u(t)$  with respect to  $t$ :  $u'(t)$ , approximated by straight lines.  
 c - The second derivative of  $u(t)$  with respect to  $t$ :  $u''(t)$ .  
 d - The third derivative of  $u(t)$  with respect to  $t$ :  $u'''(t)$ .

(Fig. 32d). Now we look again at Eq. (42). If integrated by parts this equation transforms into:

$$G(j\omega) = \frac{u(0)}{j\omega} + \frac{u'(0)}{(j\omega)^2} + \frac{u''(0)}{(j\omega)^3} + \frac{1}{(j\omega)^3} \int_0^{\infty} u'''(t)e^{-j\omega t} dt \quad (43)$$

From Fig. 32 we know that  $u(0) = 0$ ,  $u'(0) = +18$  and  $u''(0) = -280$ , while  $u'''(t)$  is represented by a set of impulses of various heights. Thus Eq. (43) may be solved at once:

$$G(j\omega) = \frac{18}{(j\omega)^2} - \frac{280}{(j\omega)^3} + \frac{1}{(j\omega)^3} \left[ 280 e^{-j\omega 0.1} + 100 e^{-j\omega 0.12} - 84 e^{-j\omega 0.208} - 16 e^{-j\omega 0.28} \right]$$

which is the same as:

$$G(j\omega) = \frac{1}{\omega^3} \left[ -280j - 18\omega + 280je^{-j\omega 0.1} + 100je^{-j\omega 0.12} - 84je^{-j\omega 0.208} - 16je^{-j\omega 0.28} \right] \quad (44)$$

To separate the real and the imaginary parts, the exponentials in Eq. (44) are written in rectangular form:

$$G(j\omega) = \frac{1}{\omega^3} (a + bj), \text{ where}$$

$$a = 280 \sin \omega 0.1 + 100 \sin \omega 0.12 - 84 \sin \omega 0.208 - 16 \sin \omega 0.28 - 18 \omega$$

$$b = -280 + 280 \cos \omega 0.1 + 100 \cos \omega 0.12 - 84 \cos \omega 0.208 - 16 \cos \omega 0.28$$

Now the amplitude-frequency and phase-frequency characteristics  $B(\omega)$  and  $\varphi(\omega)$ , respectively (cf. Eq. 13), can be found easily according to:

$$B(\omega) = \frac{\sqrt{a^2 + b^2}}{\omega^3} \text{ and } \varphi(\omega) = \text{tg}^{-1} \frac{b}{a}$$

First the values of  $a$  and  $b$  are calculated for various  $\omega$ . The results are presented in Table VI. With regard to these calculated values we note that the errors for the lowest and highest values of  $\omega$  are rather big.

$\nu$	$\omega$	$a$	$b$	$\varphi$	$B$
1	6.28	+ 23.1	+ 0.35	0°	0.093
2	12.56	+ 103	- 100	44°	0.072
4	25.1	- 211	- 657	108°	0.044
6	37.7	- 1012	- 518	153°	0.021
8	50.2	- 1141	- 56	177°	0.009
10	62.8	- 1062	- 48	178°	0.0043

Table VI.

To see what happens if  $\omega \rightarrow 0$ , we write Eq. (42) in rectangular form:

$$G(j\omega) = \int_0^{\infty} u(t) \cos \omega t dt - j \int_0^{\infty} u(t) \sin \omega t dt \quad (45)$$

Consequently: 
$$\lim_{\omega \rightarrow 0} B(\omega) = \int_0^{\infty} u(t) dt \quad (46)$$

and 
$$\lim_{\omega \rightarrow 0} \varphi(\omega) = 0 \text{ degrees} \quad (47)$$

The integral in Eq. (46) has already been evaluated for Eq. (27), where it was found that  $B(0) = \int_0^{\infty} u(t) dt = 0.1165$ .

The high-frequency behaviour can be found from the coefficients  $a$  and  $b$ .

$\lim_{\omega \rightarrow \infty} a = -\infty$  and  $\lim_{\omega \rightarrow \infty} b$  does not exist, but  $b(\omega)$  is limited for all values of  $\omega$ .

Thus:

$$\lim_{\omega \rightarrow \infty} B(\omega) = 0 \text{ and } \lim_{\omega \rightarrow \infty} \varphi(\omega) = -180 \text{ degrees.}$$

Keeping these results in mind, plots are made of  $B(\nu)$  and  $\varphi(\nu)$  in Fig. 33a and b ( $\omega = 2\pi\nu$ ).

Now we come to the solution of Eq. (41). All the double-frequency terms in Eq. (41) are at least a factor  $\rho$  less than the corresponding single frequency terms. Consequently we assume that these terms may be neglected if  $\rho$  is chosen sufficiently small.

Then Eq. (41) becomes:

$$H(t) = \frac{126.5 I_0 (1 + \rho \sin \omega t)}{\left(1 + \frac{5I_0}{7.2}\right) \left(1 + \frac{0.1I_0}{7.2}\right) + \frac{\rho I_0}{\omega^2 + 52} (36.7 + I_0) \sin \omega t - \frac{\omega \rho I_0}{\omega^2 + 52} (5.1 + 0.139I_0) \cos \omega t} \quad (48)$$

If again all terms with second or higher powers of  $\rho$  are neglected, Eq. (48) can be transformed into:

$$H(t) = \frac{126.5 I_0 (1 + \rho \sin \omega t)}{\left(1 + \frac{5I_0}{7.2}\right) \left(1 + \frac{0.1I_0}{7.2}\right)} \times \left[ 1 - \frac{\frac{\rho I_0}{\omega^2 + 52} (36.7 + I_0) \sin \omega t - \frac{\omega \rho I_0}{\omega^2 + 52} (5.1 + 0.139I_0) \cos \omega t}{\left(1 + \frac{5I_0}{7.2}\right) \left(1 + \frac{0.1I_0}{7.2}\right)} \right] \quad (49)$$

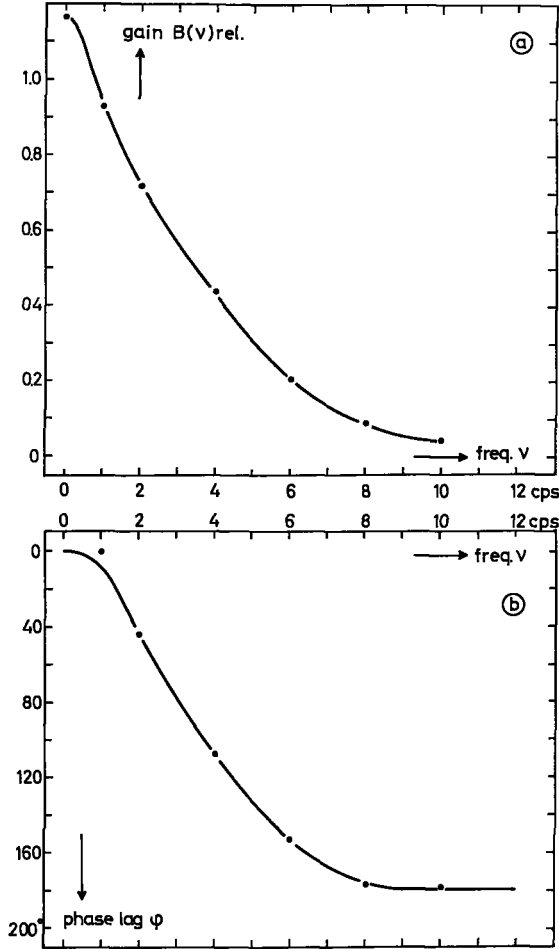


Fig. 33a - The gain  $B(v)$  of the linear system calculated from table VI.  
 b - The phase lag  $\varphi(v)$  of the linear system calculated from table VI.

Since we are not interested in the dc-component of  $H(t)$ , but only in the time-varying part, Eq. (49) can be reduced to:

$$P(t) = X \sin \omega t + Y \cos \omega t, \quad (50)$$

$$\text{where } X = \frac{126.5qI_0}{\left(1 + \frac{5I_0}{7.2}\right)\left(1 + \frac{0.1I_0}{7.2}\right)} - \frac{126.5qI_0^2(36.7 + I_0)}{(\omega^2 + 52)\left(1 + \frac{5I_0}{7.2}\right)^2\left(1 + \frac{0.1I_0}{7.2}\right)^2}$$



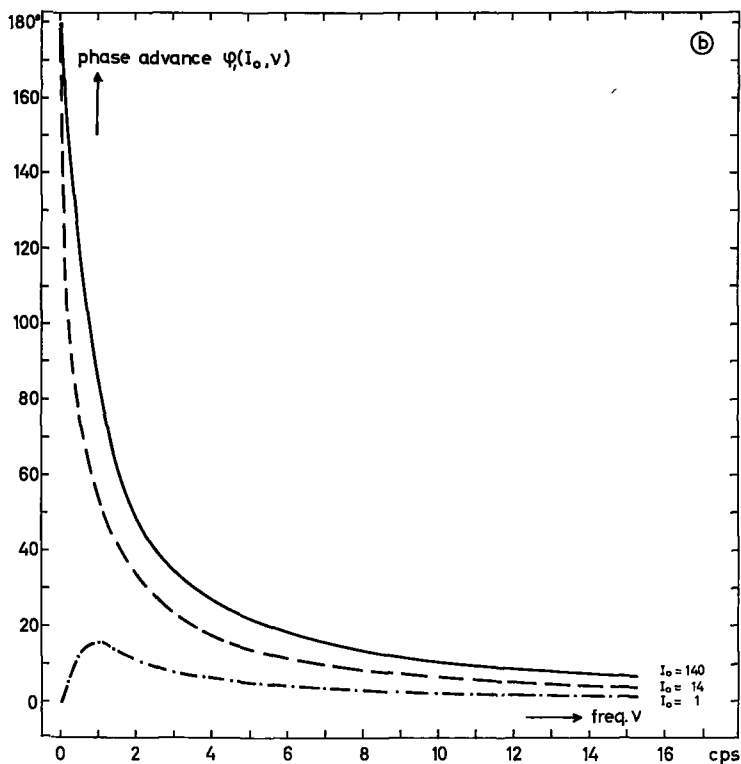
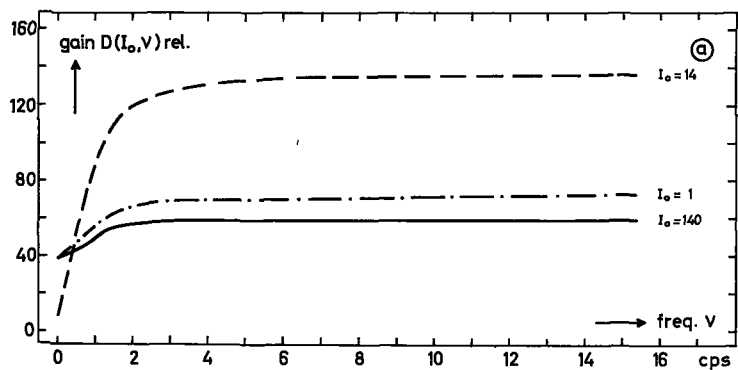


Fig. 34a - The gain  $D(I_0, \nu)$  of the non-linear system calculated according to Eq. (51).

b - The phase advance  $\varphi_1(I_0, \nu)$  of the non-linear system calculated according to Eq. (52).

$I_0$  in normalised intensity units.

$$\text{and } Y = \frac{126.5 \rho \omega I_0^2 (5.1 + 0.139 I_0)}{(\omega^2 + 52) \left(1 + \frac{5 I_0}{7.2}\right)^2 \left(1 + \frac{0.1 I_0}{7.2}\right)^2}$$

From Eq. (50) the gain  $D(I_0, \omega)$  for the fundamental frequency can be calculated as:

$$D(I_0, \omega) = \frac{1}{\rho} \sqrt{X^2 + Y^2} \quad (51)$$

And for the phase shift of the fundamental component we find:

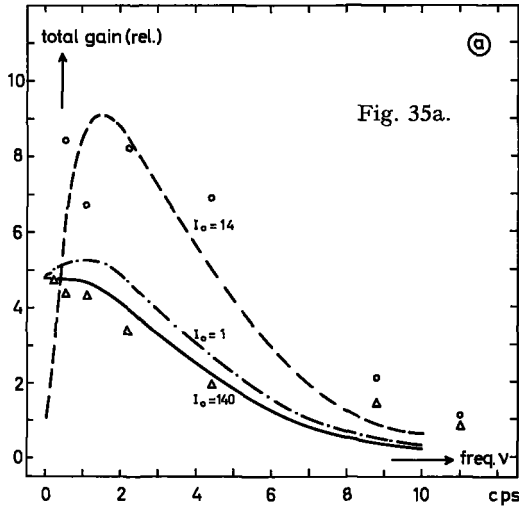
$$\varphi_1(I_0, \omega) = \text{tg}^{-1} \frac{Y}{X} \quad (52)$$

Now we will calculate  $D(I_0, \omega)$  and  $\varphi_1(I_0, \omega)$  for  $I_0 = 1$ ,  $I_0 = 14$  and  $I_0 = 140$ , and various frequencies. The result is shown in Fig. 34a and b. According to Eq. (15) and (16) the total gain and total phase shift of the system as a whole is given by:

$$\text{total gain} = B(\nu) \times D(I_0, \nu)$$

$$\text{total phase shift} = \varphi(\nu) + \varphi_1(I_0, \nu)$$

Here  $D(I_0, \nu)$  and  $\varphi_1(I_0, \nu)$  are given in Fig. 34a and b, while  $B(\nu)$  and  $\varphi(\nu)$  are given in Fig. 33a and b. The total gain and total phase shift, calculated according to these equations is shown in Fig. 35a and b.



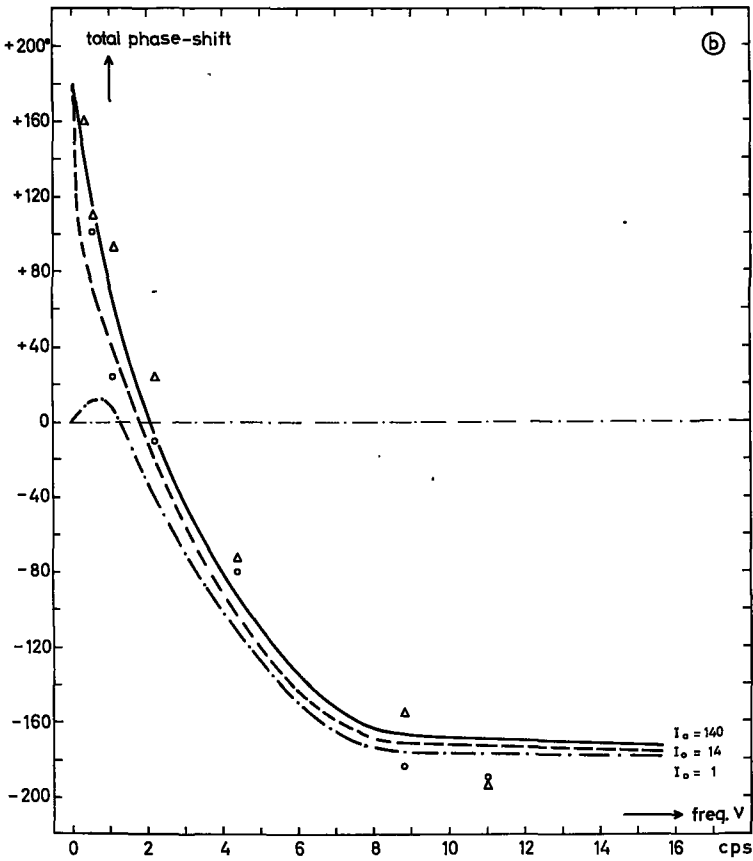
Now we want to compare these theoretical results with experimental data. Therefore, an experiment is done, in which the eye is stimulated with sinusoidally modulated light:  $I(t) = I_0 (1 + \rho \sin \omega t)$ . Two values for  $I_0$  are chosen,  $I_0 = 14$  and  $I_0 = 140$  normalised intensity units. The response of the eye is so small that in the direct

Fig. 35a - Total gain as a function of the frequency for three intensities.

- measured points for  $I_0 = 14$
- △ measured points for  $I_0 = 140$
- $I_0$  is measured in normalised intensity units.

b - Total phase shift as a function of the frequency for three intensities.

- measured points for  $I_0 = 14$
- △ measured points for  $I_0 = 140$
- $I_0$  is measured in normalised intensity units.



recordings a response can hardly be distinguished, the response has about the same amplitude as the noise. Therefore, the average response computer is used in all these experiments. The sine-wave is obtained from a function generator which also produces a synchronisation pulse, exactly at the tops of the sine-wave.

The amplitude of the sine-wave and the bias of the projection TV tube are adjusted in order to get the proper average intensity and modulation depth. The synchronisation pulse starts the average response computer, and the analysis time of this computer is set at such a value that at each frequency at least two tops of the sine-wave fall within the analysis period.

The modulation depth, i.e. the value of  $\rho$ , should not be too small because of the low response amplitude. On the other hand  $\rho$  should not be too large because of the double frequency terms which can no longer be neglected. We found that a value of  $\rho = \frac{1}{4}$  is a good compromise.

In order to get a stable base line, a time-constant of 2 sec was used in combination with the dc-chopper amplifier. Even for the lowest frequency this means a correction of less than 10% for the phase and less than 2% for the amplitude.

There is another important fact we would like to mention. In the previous part of this thesis the latency was treated as a transportation lag and left out of consideration. The response could always be shifted back so that no lag occurred between stimulus and response. As soon as we have a continuous varying stimulus like a sine-wave, this latency will give a contribution to the phase which cannot be neglected. This phase lag increases linearly with the frequency and can be calculated easily according to:

$$\nu \text{ (in cps)} \times \text{latency (in sec)} \times 360^\circ = \text{phase lag contribution} \\ \text{(in degrees).}$$

Here it is assumed that the latency is independent of the frequency  $\nu$ . By stimulating the eye with block-stimuli of the same modulation depth and average intensity, we found that for  $I_0 = 14$  the latency = 45 msec and for  $I_0 = 140$  the latency = 30 msec.

Some of the averaged *ERG* responses are shown in Fig. 36. Also the averaged response to the light stimulus of a photo cell instead of the eye is shown. This gives an idea of the synchronisation of the computer with respect to the stimulus. The analysis time and the number of averaged responses are mentioned in all situations.

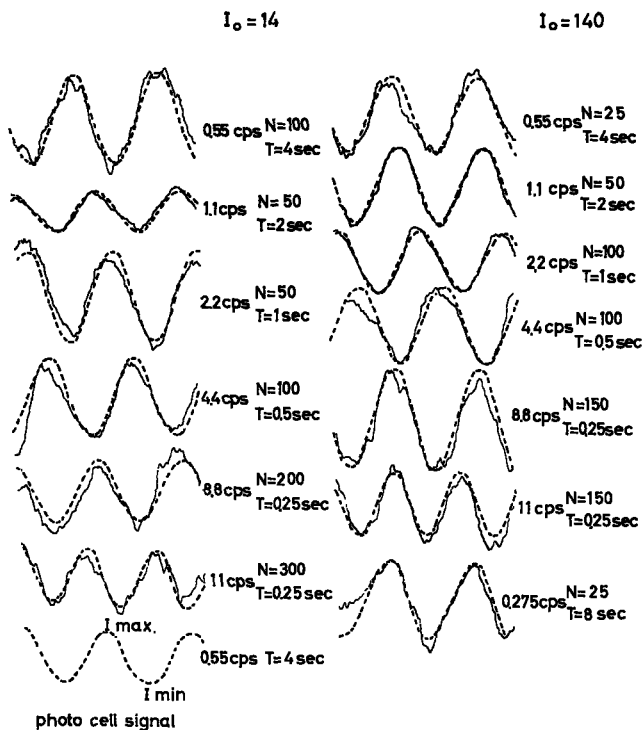


Fig. 36 - Averaged responses to sinusoidal stimulation:  $I_0(1 + \rho \sin \omega t)$ .

$N$  = number of averaged responses.

$T$  = analysis time of the average response computer.

$\rho$  =  $1/4$

----- actual sine-waves of the same amplitude and frequency as the corresponding experimental recordings.

The phase shift, measured from Fig. 36 and adjusted for the latency time is plotted in Fig. 35b, and compared with the corresponding calculated phase curves. The agreement is good, especially if we consider the big experimental error which is of the order of  $\pm 20^\circ$ .

The amplitudes of the averaged sine-waves in Fig. 36 depend on the number of responses, as well as on the analysis and the display sensitivity of the average response computer. They are not reproduced in Fig. 36 with correct relative amplitudes.

Furthermore, we noted that the contribution of successive equal groups of responses to the average response was not always the same. This indicates that the eye does not produce an output signal of very constant amplitude under these conditions. This makes the deter-

mination of the real amplitude of the *ERG* response difficult and inaccurate. It is probably the reason for the rather bad agreement between calculated and measured gain curves in Fig. 35a. The experimental points in Fig. 35a are taken from Fig. 36 and corrected for the various scale settings of the average response computer. It is clear that the phase will not be affected by an inconstancy in amplitude of the *ERG* signal, as long as the latency time is amplitude independent.

#### D. The behaviour of the light-adapted eye

So far, we always assumed the eye to be dark-adapted at the beginning of each stimulus. In this section we will investigate what happens if an originally dark-adapted eye is adapted to not-too-high intensities of a blue colour. Such an adaptation light may be regarded as a block-shaped stimulus of infinite duration.

The problem is now to calculate the response to a stimulus which is superimposed on such a long adaptation stimulus, as shown in Fig. 37.

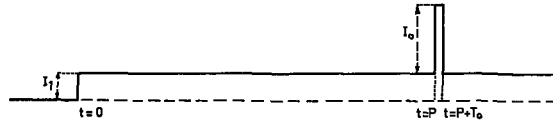


Fig. 37 - Adaptation stimulus of intensity  $I_1$ , with a block-stimulus of intensity  $I_0$  superimposed on it.  
Adaptation stimulus starts at  $t = 0$ .  
Block-stimulus starts at  $t = P$ , with  $P \gg 0$ .

We consider the situation, where the superimposed stimulus is of a short duration  $T_0$  and has an intensity  $I_0$ . According to Eq. (24) and (25) it can be shown that the response to this stimulus is equal to:

$$R(T) = R_1(T) + R_2(T) + R_3(T), \text{ where} \quad (53)$$

$$R_1(T) = \frac{126.5 I_1}{(1 + 0.695 I_1) (1 + 0.0139 I_1)} \int_T^\infty u(x - P) dx \quad (a)$$

$$R_2(T) = 60 \frac{I_1 + I_0}{I_0} \log \left[ \frac{(1 + 0.695 I_0 + 5 I_0 T_0) (1 + 0.0139 I_1)}{(1 + 0.0139 I_0 + 0.1 I_0 T_0) (1 + 0.695 I_1)} \right] u(T - P) \quad (b)$$

$$R_3(T) = \int_0^{T-P} \frac{126.5 I_1 u(T - P - t') dt'}{(1 + 0.695 I_1 + 5 I_0 T_0 e^{-7.2 t'}) (1 + 0.0139 I_1 + 0.1 I_0 T_0 e^{-7.2 t'})} \quad (c)$$

In Eq. (53) it is assumed that  $P \gg 0$        $t' = t - P - T_0$   
 $T_0 \approx 0$        $u(x) = 0$  for  $x \leq 0$ .

$I_1$  = intensity of the adaptation background in normalised intensity units.

$I_0$  = intensity of the superimposed stimulus in normalised intensity units.

$T_0$  = duration of the block-stimulus in seconds.

$u(x)$  = unit-response.

$R(T)$  = *ERG* response in % of the maximum obtainable  $B_s$ -wave in the dark-adapted eye.

Eq. (53) is solved for  $I_1 = 3.8$  normalised intensity units and  $I_0 T_0 = 1.05$ ,  $I_0 T_0 = 3.5$  and  $I_0 T_0 = 10.5$  normalised energy units. This can be done most easily numerically in the same way as demonstrated in the previous sections. The results are shown in Fig. 38, and can be understood in the following way. Before the superimposed stimulus is presented, the eye has come to a steady state ( $P \gg 0$ ), and the adaptation light causes a dc-component in the *ERG* response. The value of this dc-component at  $t = P$  is given by Eq. (53a). At  $t = P$  the stimulus to the eye is a short flash of intensity  $I_0 + I_1$  and duration  $T_0$ .

However, the past history, i.e. the long adaptation stimulus of intensity  $I_1$  must be taken into account. This is done in Eq. (53b). Finally, at  $T = P + T_0 \approx P$  the stimulus is again the adaptation light only, but now the past history is the long adaptation light before  $T = P$  and a flash of energy  $(I_0 + I_1)T_0$  at  $T = P$ . This contribution to the response is given by Eq. (53c).

The total response is the sum of the contributions given in Eq. (53a), (53b) and (53c).

There are three important differences between the light- and dark-adapted situation, as can be seen in Fig. 38.

First, the amplitude of the positive deflection in the light-adapted situation is lower than the amplitude of the response to the same flash of the dark-adapted eye.

Second, the duration of the positive deflection in the light-adapted situation is shorter than the duration of the  $B_s$ -wave, or unit-response, of the dark-adapted eye.

However, the most striking difference is the negative deflection, with a time constant of about 0.4 sec, that occurs in the response of the light-adapted eye.

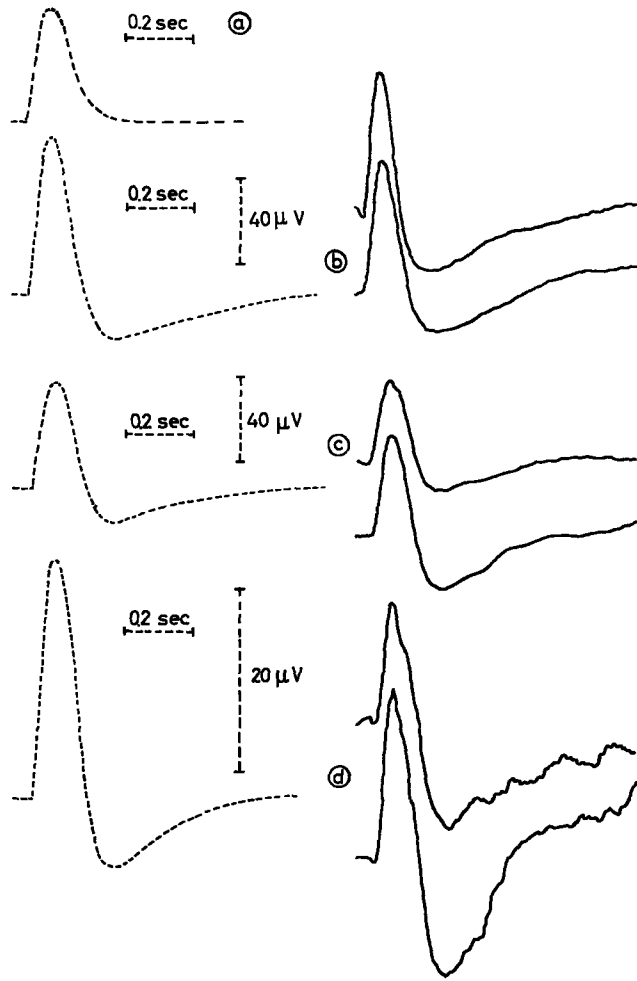


Fig. 38a - The unit-response  $u(t)$ , i.e. the ERG response of the dark-adapted eye.

- b - Calculated (-----) and experimental responses for  $I_1 = 3.8$  (adaptation) and  $I_0T_0 = 10.5$  (flash).
- c - Calculated (-----) and experimental responses for  $I_1 = 3.8$  and  $I_0T_0 = 3.5$ .
- d - Calculated (-----) and experimental responses for  $I_1 = 3.8$  and  $I_0T_0 = 1.05$ .  
 $T_0 = 0.035$  sec  
 $I_1$  is measured in normalised intensity units.  
 $I_0T_0$  is measured in normalised energy units.

(continued on page 67)



It follows from Fig. 38 that at these points there is at least a good qualitative agreement between calculated and experimental recordings. It is difficult to indicate the errors in the quantitative relationships. Both the calculated and experimental responses have their errors, caused, for instance, by an inaccuracy in the determination of the normalised intensity values of both adaptation source and flash, by possible errors in the determination of the weighting function  $g(d) = e^{-7.2d}$ , by possible inconstancy of the eye as a voltage generator, and so on.

Of course all the calculations and measurements done in the previous sections for the dark-adapted eye can be repeated for the light-adapted eye. We will not do this, but leave it with this example of a short flash on an adaptation background, which shows that such an approach is very good indeed.

(continuation underline of fig. 38).

The time and the  $\mu\text{V}$  calibrations in b) c) and d) hold for the calculated responses as well as for the experimental ones.

The experimental recordings are the average of about 20 responses. Each experiment is done twice, to get an idea of the experimental errors.

Stimulus colour (adaptation and flash) blue.

Time constant of the recording equipment 2 sec.

## CHAPTER VI

### DISCUSSION

In the foregoing chapters the electrical response of the human eye to stimulation with light has been analysed in a quantitative way under certain restricted conditions. These restricted conditions are a blue stimulus colour and a low to moderate stimulus intensity. It appeared to be possible to explain certain characteristics of this electrical response on the basis of a model, where, in a first stage, a non-linear system operates on the stimulus, followed by a linear operation in a second stage. The motivation for this arrangement of the non-linear and linear elements is the conservation of the general shape of the response of the dark adapted eye when it is stimulated with short flashes over a considerable range of intensities. Although it is impossible to give a general proof, it is felt that this conservation can never be achieved with a reversed arrangement of the linear and non-linear elements.

On the other hand, the validity of Talbot's law is often used as an argument that, at least for the psycho-physical processing of intermittent visual stimuli, the eye acts as a linear system (a low-pass filter) followed by a non-linear system. According to Talbot's law it is found that an intermittent light-stimulus, which is observed as stationary (repetition frequency  $\geq$  flicker fusion frequency), gives the same brightness impression as a constant light stimulus of the same time-averaged intensity. Deviations occur at high and low intensity levels, where the sensation is less and more, respectively, than indicated by Talbot's law<sup>28</sup>.

De Lange<sup>11</sup> argues that if the signal is processed by linear and non-linear elements, and if, moreover, Talbot's law holds for the final output of the system, then either Talbot's law must hold for the non-linear elements alone, or the non-linear elements in the system are located behind a linear element with filter action (low-pass). This can be made a little more precise by representing the non-linear operation

by  $N$  and the linear operation by  $L$ . If the periodic input is  $I(t)$ , then Talbot's law states that:

$$L[\overline{N\{I(t)\}}] = L[N\{I(t)\}] \text{ or } N[\overline{L\{I(t)\}}] = N[L\{I(t)\}],$$

depending on the sequence of the non-linear and linear operations.  $\overline{I(t)}$  represents the time average of the input. The variations in  $I(t)$  are assumed to be so fast that after the non-linear and linear operations a variation in the signal can no longer be recognised. From this last condition it follows that with this "detection criterion":

$$L[N\{I(t)\}] = \overline{L[N\{I(t)\}]} = L[\overline{N\{I(t)\}}] \text{ and } N[L\{I(t)\}] = \overline{N[L\{I(t)\}]}$$

Thus we may conclude that the validity of Talbot's law implies that  $N[\overline{I(t)}] = \overline{N\{I(t)\}}$  for an arrangement  $N \rightarrow L$ , and

$$N[\overline{L\{I(t)\}}] = \overline{N[L\{I(t)\}]} \text{ for an arrangement } L \rightarrow N.$$

Now in general the relation  $N[\overline{I(t)}] = \overline{N\{I(t)\}}$  will not hold for a non-linear operation  $N$ . Suppose, for instance, that the non-linear link in the visual data processing is the relation between the frequency  $\nu$  of nerve impulses in the visual pathway, and the light intensity  $I$ . Some authors formulate this relation by  $\nu = a \log(1 + \beta I)$ , where  $a$  and  $\beta$  are constants. Then it can be shown easily that  $N[\overline{I(t)}] \neq \overline{N\{I(t)\}}$ . From this De Lange<sup>11</sup> concluded that an arrangement  $N \rightarrow L$  is not possible. On the other hand, if the linear operation is some sort of low-pass filter action, then at the "fusion frequency" the variation in  $L\{I(t)\}$  can be made so small that "small signal linearisation" can be applied to the non-linear operation  $N$ . This means that

$$N[\overline{L\{I(t)\}}] = \overline{N[L\{I(t)\}]}, \text{ according to Talbot's law.}$$

Now it is interesting that the model developed in this thesis for the *ERG* response accounts for Talbot's law\*. This model has an arrangement  $N \rightarrow L$  (cf. Fig. 2a) of the non-linear and linear operations. In Chpt. V, Sec. B, we have already noticed that for short flashes with a repetition frequency  $\nu > 20$  cps, the dc-component in the steady state *ERG* response is the same as that which is observed with a constant light stimulus of the same average intensity. This followed both from experiments and from predictions with the model, indicating that

\* I am very much indebted to Dr. R. DeVoe (John Hopkins University, School of Medicine, Baltimore, U.S.A.) for drawing my attention to this possible discrepancy between my model and De Lange's model.

Talbot's law holds for the electro-retinographic response. Consequently, for the non-linear operation  $N$  in our model we must find:

$$N\{\overline{I(t)}\} = \overline{N\{I(t)\}}.$$

We will show this more explicitly on the basis of an example. Suppose the input  $I(t)$  to the non-linear element is a series of block-pulses (intensity  $I_0$ , duration  $T_0$ ) of repetition frequency  $\nu$ . The output of the non-linear element is  $H(t)$  (cf. Eq. (24)), where

$$H(t) = \frac{126.5 I(t)}{(1 + 5 \int_0^t I(\tau) e^{-7.2(t-\tau)} d\tau) (1 + 0.1 \int_0^t I(\tau) e^{-7.2(t-\tau)} d\tau)}$$

From this we calculate in the steady state:

$$N\{\overline{I(t)}\} = \frac{126.5 \nu I_0 T_0}{(1 + 0.695 \nu I_0 T_0) (1 + 0.0139 \nu I_0 T_0)}$$

and

$$\overline{N\{I(t)\}} = \int_0^{T_0} \left[ \frac{126.5 \nu I_0}{1 + 0.695 I_0 \left\{ e^{-7.2t'} \left( \frac{e^{-7.2(t'/\nu - T_0)} - 1 \right)} + 1 \right\}} \right] \times \left[ \frac{1}{1 + 0.0139 I_0 \left\{ e^{-7.2t'} \left( \frac{e^{-7.2(t'/\nu - T_0)} - 1 \right)} + 1 \right\}} \right] dt'$$

Now it can be shown that within the experimental error

$$N\{\overline{I(t)}\} = \overline{N\{I(t)\}} \text{ for a repetition frequency } \nu > 20 \text{ cps.}$$

Summarizing, we conclude that for a non-linearity which only depends on the amplitude of the input, Talbot's law does not hold. If, in addition, the non-linearity is time dependent (energy storage, adaptation effects) it is possible that in a particular situation Talbot's law is valid.

The effect of the non-linear system developed in this *ERG* model, shows many similarities with light- and dark-adaptation. The non-linear operation could be described by  $H(t) = I(t)S$ , where  $H(t)$  is the output of the non-linear element,  $I(t)$  is the input and  $S$  is a variable sensitivity, the value of which is dependent on the past history of the input:

$$S = S \left[ \int_0^t I(\tau) g(t - \tau) d\tau \right]$$

Here  $g(t)$  is a weighting function, and for the electro-retinographic system  $g(t)$  could be approximated by  $g(t) = e^{-7.2t}$ . However, one must be very careful in identifying  $S$  with the adaptive state of the eye, since the introduction of this sensitivity  $S$  is more or less operational, and is based on the electrical behaviour of the eye only.

In the literature several models for signal processing in the eye have been developed to account for the psycho-physical or electrical data.

Well-known is the already-mentioned model by De Lange<sup>11</sup> for psycho-physical flicker fusion experiments. The non-linear aspects of this model are left out of consideration, because the "small signal linearization" is an essential tool in this kind of systems analysis.

Kelly's<sup>25</sup> model describes some psycho-physical flicker-fusion data (the field configuration is different from the one used by De Lange), as well as some electrical responses to transients of light. In fact, Kelly extrapolates his model, which is based on photopic psycho-physical experiments, to explain some electrical phenomena. In this way he calculates a step response, which shows much resemblance with the electro-retinographic *A*-wave and *X*-wave. These are rather fast photopic waves.

Both models have in common that the first stage is a linear operation working on some analog basis (continuous output), followed by a non-linear second stage working on a more or less digital basis (pulse output).

Van der Tweel<sup>37</sup> was the first one to show that with a sinusoidally modulated light stimulus superimposed on a constant background, the human *ERG* response is a sine-wave too, if the modulation depth is not too high. With the same "small signal linearizations" as used by De Lange, Van der Tweel calculated impulse- and step-responses from the measured frequency characteristics.

Such a linear analysis has also been applied to more primitive visual systems by DeVoe<sup>12</sup>, and Hermann and Stark<sup>21</sup>.

The model developed in this thesis works on an analog basis (the non-linear as well as the linear operation), and has been derived from scotopic *ERG* data. It starts with a non-linear operation and is assumed to be situated at the very beginning of the visual process. This can be motivated by the general assumption that the *ERG* is a primary visual reaction, or at least the by-product of such a primary reaction.

Some attempts were made to extrapolate this model to psycho-physical experiments, for instance, to calculate the flicker fusion frequency as a function of the stimulus intensity (cf. Chpt. V, Sec. A), and to calculate attenuation characteristics, analogous to those obtained by De Lange<sup>11</sup> (cf. Troelstra and Schweitzer<sup>34</sup>). Although the obtained results are promising, much more work has to be done to establish the exact relationships.

As another point of interest we mention the "critical duration", defined as the duration of a flash of light above which the flash intensity is the determining variable and below which the product of intensity and duration is the determining variable. Graham and Margaria<sup>17</sup> noted that this critical duration is a little more than 100 msec for psycho-physical threshold excitations in the dark-adapted eye. They found that a decrease in the area of the retinal image results in a more abrupt transition from one determining variable to the other near the critical duration. This is attributed to a statistical distribution of properties among a large number of sensory cells. Johnson and Bartlett<sup>24</sup> describe experiments where the  $B_s$ -wave amplitude is measured as a function of the stimulus duration and stimulus intensity for a visual field of about  $7.5^\circ$  (Maxwellian view). They also found a maximum critical duration of about 100 msec in the dark-adapted eye for the lowest stimulus intensities. These findings were confirmed by Alpern and Faris<sup>1</sup> and by own measurements (cf. Chpt. IV, Sec. A).

Besides this our model yielded a set of calculated amplitude versus duration curves (stimulus intensity as a parameter) very similar to those of Johnson and Bartlett<sup>24</sup> (cf. Fig. 15). These authors note that for an adaptation to 0.02 ft-L the maximum critical duration for the  $B_s$ -wave becomes shorter, having a value of about 30 msec. There are qualitative indications that our model will account for this decrease of the critical duration in the light-adapted eye. In Chpt. V, Sec. D some calculated and measured responses to short flashes on an illuminated background are shown (cf. Fig. 38). The time from the beginning of the response to the first zero-crossing becomes shorter if a background is present. Since the critical duration depends strongly on that time, a similar effect can be expected for the critical duration. Calculations on this point are very laborious and so far we do not have any quantitative results.

The possibility of describing the critical duration and its dependence on the adaptation level is an interesting aspect of this model, since no digitalization of the information (transformation to spikes) has occurred.

We conclude this chapter with some remarks about the effect of the non-linear operation in the visual system on the perception of time-varying light stimuli. One can think, for example, about the possibility of perceiving beats if the eye is stimulated with two signals of different frequencies. A connection can be made here with another field of investigation, the stimulation of the eye by electric current. If an alternating electric current is applied to the human body by means of two electrodes (one of them is usually placed near the eye), a light-flicker can be noted which is called the electric phosphene. The minimum current necessary to evoke such an electric phosphene depends on the frequency of the stimulating current. For low frequencies ( $\nu < \text{about } 5 \text{ cps}$ ) and high frequencies ( $\nu > \text{about } 100 \text{ cps}$ ) the eye is rather insensitive, but in the range from 20-40 cps a maximum sensitivity for this kind of stimulation exists. Crapper and Noell<sup>10</sup> found that electric stimulation of a rabbit eye with short trans-retinal pulses yielded responses of the retinal ganglion cells. These responses consisted of 2 or 3 bursts of spikes separated by equal intervals of time and with a decreasing number of spikes in each successive burst – a possible indication of a damped oscillation. For a subliminal conditioning stimulus, followed after a variable time by a test stimulus, they found an alternation of facilitation and inhibition of the test stimulus, depending on the separation of the two pulses. This change between facilitation and inhibition also resembled a damped oscillation and with the same time constants. Calculations using an excitability curve for sinusoidal currents of variable frequencies, and assuming a linear operation, resulted in a resonant frequency and damping coefficient of the pulse response in fair agreement with the experimental results.

Bouman and Ten Doesschate<sup>3</sup> found that experimental excitability curves of the human eye for sinusoidal and pulse-shaped currents could be calculated from each other with the use of linear operations only. These are indications that the system one can think of as existing between input-current and output-phosphene is linear for near-threshold excitations.

Brindley<sup>6</sup> reports some experiments on interaction between varying light stimuli and alternating electric current produced by simultaneous stimulation. His results can be summarized as follows: Light pulses of frequency  $n$  (light/dark ratio usually 1/15) interact with a sinusoidal electrical current of frequency  $a(n + \delta n)$  ( $a = 1, 2, \dots, 11$ ) resulting in beats of frequency  $a\delta n$ . For instance, light of 100 cps, which is seen

as stationary (frequency above flicker fusion frequency), can give beats with a current of 101 cps. Also light of about 40 cps can give beats with a current of 441 cps. If  $a = 1/2$ , beats could be seen, but Brindley never observed beats if  $a = 1/3, 1/4, \dots$

These results might indicate that the light pulses generate a considerable number of higher harmonics (up to about 10) which can interact with currents of nearly the same frequencies. On the other hand, an electrical current (pulsed or sinusoidal) obviously generates a first harmonic only, and the beats between this first harmonic and light of the same frequency are less clear. This is in agreement with the already mentioned proposal that the electrical current is probably processed more or less linearly. The brightness levels in Brindley's experiments were photopic. This, and the fact that pulsed light is used, make a comparison with our model difficult.

For sinusoidal stimulation above the flicker fusion frequency our model predicts that the generation of higher harmonics in the *ERG* is negligible.

In a psycho-physical experiment we found that two light stimuli of nearly the same frequency ( $>$  flicker fusion frequency) do not interact and give no perceptable beats. This is, in fact, Talbot's law, which holds both for our *ERG* model and for psycho-physical experiments. It would be interesting to know how current would interact with these scotopic light stimuli, and what the interaction between two currents of different frequencies would be. If we have for instance: light – light  $\rightarrow$  no interaction, light – current  $\rightarrow$  interaction (also with higher harmonics of the light stimulus) and current – current  $\rightarrow$  no interaction, then it might be that the current acts upon the sensitivity  $S$  by which the light intensity is multiplied. In other words, the interaction would have a multiplicative character. Although these arguments are highly speculative, they provide some interesting alternatives for further experimentation.



## SUMMARY

In Chpt. I a short historical review of the origin and development of electro-retinography during the past hundred years is given. It appears that still little is known about the precise relation between variations in the light stimulus and the resulting electrical response of the human eye. This thesis deals with one aspect of this relationship, namely the effect of the light distribution in the stimulus as a function of the time. The experimental set-up consists of a stimulus generator, which transforms any voltage variation into a proportional light intensity variation by means of a television projection tube. After amplification, the electrical response of the eye can be recorded directly, or after being processed by an average response computer, depending on the signal-to-noise ratio.

In Chpt. II some aspects of non-linear systems analysis are summarized briefly. The case where the input  $I(t)$  is multiplied by a sensitivity function  $S$ , is discussed more extensively.  $S$  is supposed to depend on the past history of the input, which is characterized by a weighting function  $g(t)$ . If the system consists of a non-linear element  $n$  followed by a linear element  $l$  (cf. Fig. 2a), it is shown how the sensitivity function  $S$  and the impulse response of the linear element can be determined from an experiment with short single input pulses, and how the weighting function  $g(t)$  can be found from an experiment with double-pulses. Finally the system response to sinusoidal stimulation is studied.

In Chpt. III the electrical response of the dark-adapted human eye is investigated, and some non-linearities in the relation between this response and the light stimulus are indicated.

Under restricted stimulus conditions, namely a blue stimulus of low to moderate intensities, the response to short light flashes consists of a slow positive wave, the scotopic  $B_s$ -wave.

Some analogies between this  $B_s$ -wave and the pulse response of the

non-linear system developed in Chpt. II are pointed out. This forms the basis for a model of the electro-retinographic system. The light stimulus  $I(t)$  is processed first by a non-linear element in which  $I(t)$  is multiplied by a sensitivity function

$$S = S \left[ \int_0^t I(\tau) g(t - \tau) d\tau \right], \text{ where } g(t) \text{ is a weighting function.}$$

After this the signal is processed further by a linear element.

The sensitivity function  $S$ , the weighting function  $g$  and the pulse response of the linear element are determined for the electro-retinographic system by stimulating the dark-adapted eye with single and double flashes of light.

In the chapters IV and V the model is tested under various experimental conditions. Single stimuli are considered first: block-stimuli of various durations, the step-function and the ramp-function. In all these situations the *ERG* response is calculated, with the intensity as a parameter. Corresponding experiments show a good agreement with these calculations. The same procedure is followed with repetitive stimuli: series of short flashes and sinusoidally modulated light intensities. For the sinusoidal stimulation, the contributions of the non-linear and linear elements to the phase-frequency and gain-frequency characteristics, are calculated separately.

One of the results is the prediction of a phase-advance for the lowest frequencies which can amount to as much as  $180^\circ$ , depending on the average intensity level. Here again experiments provided a nice confirmation of the predictions based on the model.

It is also possible to investigate the effect of light-adaptation on the *ERG* response. The drastic change in response which occurs if a flash is presented on a light background instead of to a completely dark-adapted eye can be predicted by the model.

Finally, in Chpt. VI possible relationships between the electro-retinographic model and some psycho-physical experiments are discussed. Examples are the law of Talbot, the critical duration in relation to temporal summation, and interactions between intermittent light stimulation (flicker) and stimulation with alternating current (phosphene).

Although these relations are still vague and ill-defined, it is felt that there are many possibilities for further investigation.

## SAMENVATTING

In hoofdstuk I wordt eerst een kort historisch overzicht gegeven over het ontstaan en de ontwikkeling van de electro-retinografie gedurende de laatste honderd jaar. Het blijkt, dat nog steeds weinig bekend is over de juiste relatie tussen de veranderingen in de lichtprikkel en de hierdoor optredende elektrische responsies in het menselijk oog. Dit proefschrift behandelt een bepaald aspect van deze relatie, namelijk het effect van de temporale lichtdistributie in de stimulus.

De meetapparatuur, die vervolgens wordt besproken, bestaat uit een stimulus-generator, versterker en registreer-apparatuur. In de stimulus-generator wordt een spanningsvariatie in een evenredige variatie van de lichtintensiteit getransformeerd, door middel van een projectie-televisiebuis. Na versterking kan de elektrische responsie van het oog direct geregistreerd worden, of het gemiddelde van een aantal identieke responsies kan bepaald worden met behulp van een speciaal voor dit soort metingen geschikte digitale rekenmachine, ter verbetering van de signaal-ruis verhouding.

In hoofdstuk II zijn enkele aspecten van de niet-lineaire systeem analyse kort samengevat. Meer uitgebreid wordt het geval besproken waar het ingangssignaal  $I(t)$  vermenigvuldigd wordt met een gevoeligheidsfunctie  $S$ . Deze functie  $S$  wordt verondersteld van de „voorgeschiedenis” van het ingangssignaal af te hangen op een wijze die beschreven kan worden met een gewichtsfunctie  $g(t)$ . Voor het geval dat het systeem bestaat uit een niet-lineair element  $n$ , gevolgd door een lineair element  $l$  (vgl. Fig. 2a), wordt besproken hoe de gevoeligheidsfunctie  $S$  en de impuls responsie van het lineaire element bepaald kunnen worden uit een experiment met korte ingangspulsen. De gewichtsfunctie  $g(t)$  kan gevonden worden door ingangspulsen op variabele tijdsafstand te gebruiken. Tenslotte wordt de responsie van het systeem op sinusvormige ingangssignalen bestudeerd.

In hoofdstuk III is de elektrische responsie van het donkergeadapteerde

menselijke oog onderzocht, en enkele niet-lineaire eigenschappen in de relatie tussen deze responsie en de lichtprikkel worden aangeduid. Onder bepaalde stimuluscondities, zoals een blauwe kleur en lage tot middelmatige helderheden, bestaat de responsie op een korte lichtflits uit een langzame positieve golf, de  $B_s$ -golf. Gewezen wordt op enkele overeenkomsten tussen de aard van deze  $B_s$ -golf en de impuls responsie van het in hoofdstuk II ontwikkelde niet-lineaire systeem. Dit is de basis voor een model van het electro-retinografische systeem. De lichtstimulus  $I(t)$  wordt eerst behandeld door een niet-lineair element, waar  $I(t)$  wordt vermenigvuldigd met een gevoeligheidsfunctie  $S$ .

$$S = S \left[ \int_0^t I(\tau) g(t - \tau) d\tau \right], \text{ waar } g(t) \text{ de gewichtsfunctie voorstelt.}$$

Hierna wordt het signaal verder behandeld door een lineair element. De gevoeligheidsfunctie  $S$ , de gewichtsfunctie  $g$  en de impuls responsie van het lineaire element kunnen voor het electro-retinografische systeem geheel bepaald worden door het donkergeadapteerde oog te stimuleren met lichtflitsen van verschillende intensiteit en op verschillende tijden na elkaar aangeboden.

In de hoofdstukken III en IV wordt het model getest voor meer algemene stimuli. Eerst worden stimuli beschouwd die slechts eenmaal worden aangeboden, zoals blokvormige flitsen van verschillende duur, de stapfunctie en de functie  $I(t) = aI_0t$ . In al deze gevallen is de *ERG*-responsie berekend met de intensiteit als parameter. De experimenten stemden goed overeen met deze berekeningen. Dezelfde methode is gevolgd met herhaald aangeboden stimuli, zoals reeksen van korte flitsen en sinusvormig gemoduleerde lichtintensiteiten. Voor deze sinusvormige stimulatie zijn de bijdragen tot de fase-frequentie- en amplitude-frequentie karakteristieken van het niet-lineaire en lineaire element afzonderlijk berekend.

Een interessant resultaat is de voorspelling van een voorlopen van de fase bij de laagste frequenties, wat zelfs  $180^\circ$  kan bedragen, afhankelijk van het gemiddelde intensiteits niveau.

Ook hier geven experimenten een mooie bevestiging van de voorspellingen gebaseerd op het model.

Het is ook mogelijk de invloed van lichtadaptatie op de *ERG*-responsie te onderzoeken. De drastische verandering van de responsie in vorm en amplitude, die optreedt wanneer een flits op een lichte achtergrond wordt aangeboden, in plaats van aan een volledig donker geadaptieerd oog, kan voorspeld worden met behulp van het model.

Tenslotte worden in hoofdstuk VI mogelijke relaties tussen dit electroretinografische model en enkele psycho-fysische experimenten besproken. Voorbeelden zijn de wet van Talbot, de kritische stimulusduur in relatie tot temporale sommatie en interacties tussen intermitterende lichtstimulatie (flikker) en stimulatie met een elektrische wisselstroom (fosfeen).

Hoewel deze relaties nog vaag en slecht gedefinieerd zijn, blijven er veel mogelijkheden tot verder onderzoek.

## REFERENCES

1. ALPERN, M. and FARRIS, J. J., Luminance-duration relationship in the electric response of the human retina, *J. Optic. Soc. America* 46:845-850, 1956.
2. BERNHARD, C. G., Contributions to the neurophysiology of the optic pathway, *Acta physiol. Scand.*, Suppl. I, 1, 1940.
3. BOUMAN, M. A. and TEN DOESSCHATE, J., Personal communication.
4. BORNSCHEIN, H. and GUNKEL, R. D., The effect of rate of rise of photic stimuli on the human electro-retinogram, *Am. J. Ophth.* 42:239-243 (Oct. Pt. II), 1956.
5. BORNSCHEIN, H. and VUKOVICH, V., Das Elektoretinogram bei Mangelhemeralopie, v. Graefes *Arch. für Ophth.* 153:484-487, 1953.
6. BRINDLEY, G. S., Beats produced by simultaneous stimulation of the human eye with intermittent light and intermittent or alternating current, *J. Physiol.* 164:157-167, 1962.
7. BROWN, K. T. and WIESEL, T. N., Analysis of the intraretinal electro-retinogram in the intact cat eye, *J. Physiol.* 158:229-256, 1961.
8. BRÜCKE, E. T. V. and GARTEN, S., Zur vergleichenden Physiologie der Netzhautströme, *Arch. ges. Physiol.* 120:290-348, 1907.
9. CRAMPTON, G. H. and ARMINGTON, J. C., Area-intensity relation and retinal location in the human electro-retinogram, *Am. J. Physiol.* 181:47-53, 1955.
10. CRAPPER, D. R. and NOELL, W. K., Retinal excitation and inhibition from direct electrical stimulation, *J. Neurophysiol.* 26:924-947, 1963.
11. DE LANGE DZN., H., Relationship between critical flicker-frequency and a set of low-frequency characteristics of the eye, *J. Optic. Soc. America* 44:380-389, 1954.
12. DEVOE, R. D., Linear relations between stimulus amplitudes and amplitudes of retinal action potentials from the eye of the wolf spider, *J. of Gen. Physiol.* 47:13-32, 1963.
13. DEWAR, J. and MCKENDRICK, J. G., On the physiological Action of Light: I, *J. Anat. Physiol.* 7:275-278, 1873.
14. EINTHOVEN, W. and JOLLY, W. A., The form and magnitude of the electrical response of the eye to stimulation by light at various intensities, *Quart. J. Exper. Physiol.* 1:373-416, 1908.
15. GOODMAN, G. and ISER, G., Physiologic studies with flicker electro-retinography, *Am. J. Ophth.* 42:212-227 (Oct. Pt. II), 1956.

16. GOTCH, F., The time relations of the photoelectric changes in the eyeball of the frog, *J. Physiol.* 29:388-410, 1903.
17. GRAHAM, C. H. and MARGARIA, R., Area and the intensity-time relation in the peripheral retina, *Am. J. Physiol.* 11:299-305, 1935.
18. GRANIT, R., *Sensory mechanisms of the retina*, London, Oxford University Press, 1947.
19. GRANIT, R., The components of the retinal action potentials in mammals and their relation to the discharge of the optic nerve, *J. Physiol.* 77:207-239, 1933.
20. HENKES, H. E., v. D. TWEEL, L. H. and DENIER v. D. GON, J. J., Selective amplification of the electro-retinogram, *Ophthalmologica* 132:140-150, 1956.
21. HERMANN, H. T. and STARK, L., Single unit responses in a primitive photoreceptor organ, *J. Neurophysiol.* 26:215-228, 1963.
22. HOLMGREN, F., Method att abjectivera effecten av ljusintyck pa retina, *Upsala läkeref. förh.* 1:177-191, 1865-1866.
23. JOHNSON, E. P., The character of the B-wave in the human electro-retinogram, *A.M.A. Arch. Ophth.* 60:565-591, 1958.
24. JOHNSON, E. P. and BARTLETT, N. R., Effect of stimulus duration on electrical responses of the human retina, *J. Optic. Soc. America* 46:167-170, 1956.
25. KELLY, D. H., Visual responses to time-dependent stimuli. I. Amplitude sensitivity measurements, *J. Optic. Soc. America* 51:422-429, 1961. Visual responses to time dependent stimuli. II. Single-channel model of the photopic visual system, *J. Optic. Soc. America* 51:747:754, 1961.
26. KOCHENBURGER, R. J., A frequency response method for analyzing and synthesizing contactor servomechanisms, *Trans. AIEE Vol. 69 part I:* 270-284, 1950.
27. KÜHNE, W. and STEINER, J., Über das elektromotorische Verhalten der Netzhaut, *Unters. Physiol. Inst. Heidelberg* 3:327-377, 1880.
28. NIGHT VISION, G. E. Jayle editor, Charles C. Thomas publisher, Springfield, Ill., U.S.A.
29. PIPER, H., Über die Netzhautströme, *Arch. Physiol.* 83:85-132, 1911.
30. RIGGS, L. A. and JOHNSON, E. P., Electrical responses of the human retina, *J. Exper. Psychol.* 39:415-424, 1949.
31. SCHUBERT, G. and BORNSCHEIN, H., Beitrag zur Analyse des menschlichen Elektoretinogramms, *Ophthalmologica* 123:396-413, 1952.
32. SCHWEITZER, N. M. J. and TROELSTRA, A., On the physiological standardization of the light source in electroretinography, *Ophthalmologica* 146: 114-123, 1963.
33. SOLODOVNIKOV, V. V., *Introduction to the statistical dynamics of automatic control systems*, Dover Publications, New York, 1960.
34. TROELSTRA, A. and SCHWEITZER, N. M. J., On the relationship between the single flash ERG and the ERG on more complex stimuli, *Doc. Ophthal.*, in press.
35. TROELSTRA, A. and SCHWEITZER, N. M. J., An analysis of the B-wave in the human ERG, *Vision Res.* 3:213-226, 1963.
36. TRUXAL, J. G., *Automatic Feedback Control System Synthesis*, McGraw Hill, New York, 1955.

37. VAN DER TWEEL, L. H., Some problems in vision regarded with respect to linearity and frequency response, *Annals of the New York Academy of Sciences*, 89:829-856, 1961.
38. Vos, J. J., Personal communication.
39. VUKOVICH, V., Das ERG des Achromaten, *Ophthalmologica* 124:354-359, 1952.
40. WAGMAN, I. H., WALDMAN, J., NAIDORFF, D., FEINSCHIL, L. B. and CAHAN, R., The recording of the electro-retinogram in humans and in animals, *Am. J. Ophth.* 38 (July Pt. II):60-69, 1954.
41. WALLER, A. D., On the double nature of the photo-electrical response of the frog's retina, *Quart. J. Exper. Physiol.* 2:169-185, 1909.